THE EFFECT OF SOLUTE CONCENTRATION ON THE STRENGTH AND STRAIN AGING BEHAVIOR OF AN Al-Mg-Si SHEET ALLOY

A Thesis Submitted to the College of

Graduate Studies and Research

in Partial Fulfillment of the Requirements

for the Degree of Master of Science

in the Department of Mechanical Engineering

University of Saskatchewan

Saskatoon

By

Garett Matthew Dmytrowich

PERMISSION TO USE

In presenting this thesis/dissertation in partial fulfillment of the requirements for a Postgraduate degree from the University of Saskatchewan, I agree that the Libraries of this University may make it freely available for inspection. I further agree that permission for copying of this thesis/dissertation in any manner, in whole or in part, for scholarly purposes may be granted by the professor or professors who supervised my thesis/dissertation work or, in their absence, by the Head of the Department or the Dean of the College in which my thesis work was done. It is understood that any copying or publication or use of this thesis/dissertation or parts thereof for financial gain shall not be allowed without my written permission. It is also understood that due recognition shall be given to me and to the University of Saskatchewan in any scholarly use which may be made of any material in my thesis/dissertation.

Requests for permission to copy or to make other uses of materials in this thesis/dissertation in whole or part should be addressed to:

Head of the Department of Mechanical Engineering
57 Campus Drive
University of Saskatchewan
Saskatoon, Saskatchewan S7N 5A9
Canada

ABSTRACT

There is a strong desire among automobile manufacturers to reduce the fuel consumption and greenhouse gas emissions of their current vehicles. Reducing the overall weight of a vehicle represents the most practical opportunity to reduce fuel consumption. Replacing the current steel sheet structures with lightweight alternatives, such as aluminum, offers an excellent solution. Much of the attention in North America has been focused on copper-containing Al-Mg-Si aluminum alloys (6xxx series), such as AA6111. These alloys offer an excellent combination of good formability and precipitation-strengthening ability.

In this study, the effect of solute concentration on the strength and strain aging behavior of a proprietary Al-Mg-Si-(Cu) alloy was evaluated. The experimental design used was a 2^6 full factorial design, with the primary factors being the solute concentrations of magnesium, silicon, and copper, as well as the effects of applied strain (cold work), and natural and artificial aging heat treatments (e.g., a simulated paint bake process). The primary investigative techniques employed included tensile testing, microhardness measurements, and optical metallography.

The results show that cold work and artificial aging produce the most substantial strengthening in the alloys. The occurrence of natural aging prior to forming and artificial aging reduced strengthening. The highest strength levels in the naturally aged and paint baked condition, which most closely resembles what is found in

industry, were achieved at a combination of low magnesium levels (i.e., 0.5 wt.%) and high silicon and copper levels (i.e., 0.9 and 0.3 wt.%, respectively).

ACKNOWLEDGEMENTS

I would like to thank the entire College of Engineering and Department of Mechanical Engineering. Specifically, special thanks goes to my supervisors, professors Spiro Yannacopoulos and Ike Oguocha for their support, guidance, and assistance, as well as the members of my supervisory committee, professors Qiaoqin Yang and Akindele Odeshi. Special thanks should also be given to Dr. Alok Gupta, the industrial liaison for this project, and Novelis for supplying the materials. I would also like to thank Mr. Robert Peace and Mr. Hans Steinmetz for their immeasureable help and assistance during the research portion of this project.

I would like to thank my family and friends for their support, understanding, and encouragement.

This work was made possible by the financial support from NSERC and the Department of Mechanical Engineering, University of Saskatchewan. Without these funds, the completion of this project would not have been possible.

Thank you all.

TABLE OF CONTENTS

Permission to Use ……...…….... i

Abstract ……..... ii

Acknowledgements ……..... iv

Table of Contents …...…….. v

List of Tables ……..……... viii

List of Figures ……. ix

List of Abbreviations and Symbols …… xi

1 INTRODUCTION ……...… 1

1.1 Overview ……...……... 1

1.2 Vehicle Weight Reduction ……...…… 3

1.3 Problem Definition …….. 7

1.4 Research Objectives ……. 8

1.5 Thesis Outline …….. 8

2 LITERATURE REVIEW ……. 9

2.1 Strengthening in Metals ……... 9

2.2 Strengthening in Aluminum Alloys ……... 10

2.2.1 Grain Size Reduction …… 11
2.2.2 Strain Hardening …… 12
2.2.3 Solid Solution Strengthening …… 13
2.2.4 Precipitation Hardening …… 14

2.3 Strengthening Al-Mg-Si Alloys ……. 16

2.3.1 Precipitation Sequence of Al-Mg-Si-(Cu) Alloys ……. 17
2.3.2 Natural and Artificial Aging ……... 20

2.4 Improving the Strength of Automotive Aluminum Alloys …… 23

2.4.1 The Effect of Excess Silicon ……... 23
2.4.2 The Effect of Copper ……. 24

3 MATERIALS AND EXPERIMENTAL PROCEDURE ……... 26

3.1 Research Plan ……. 26

3.2 Materials …… 30

3.3 Experimental Procedure ……. 31

3.3.1 Thermal Processing ……... 32
3.3.2 Mechanical Properties ……... 33
3.3.3 Statistical Model Development ……. 34
3.3.4 Grain Sizing ……... 40

4 RESULTS AND DISCUSSION …… 41

4.1 Tensile Results ……... 41

4.2 Natural Aging Behavior ……. 42

4.3 Main Factors Influencing the Yield Strength of the Alloys Studied ……... 44

4.3.1 The Effect of Cold Work ……... 47
4.3.2 The Effect of Artificial Aging During the Paint Bake Cycle …….. 49
4.3.3 The Influence of Natural Aging ……. 51
4.3.4 Compositional Effects on the Yield Strength …… 55

4.4 The Factors Affecting the Paint Bake Response ……... 62

4.5 The Formability of the Alloys Studied …….. 64

4.6 The Factors Affecting Ultimate Tensile Strength …….. 65

4.7 An Examination of the Grain Morphology …… 71

5 CONCLUSIONS AND RECOMMENDATIONS ……. 74

5.1 Conclusions …… 74

5.2 Recommendations for Future Work …….. 75

REFERENCES …….. 77

APPENDICES ……... 81

A Procedure for Weck's Reagent …….. 81

B Stress-strain Curves ……... 82

C Statistics for Primary Factors ……. 89

LIST OF TABLES

Table 2.1 - The compositional limits for Al-Mg-Si alloys …… 17

Table 2.2 - Increasing yield strength with increasing silicon content ……... 25

Table 3.1 - The main parameters studied and their levels ……. 27

Table 3.2 - The 2^6 full factorial experimental design table …… 28

Table 3.3 - Chemical composition of the alloys studied ……... 31

Table 4.1 - Primary factors affecting mean yield strength …… 45

Table 4.2 - The paint bake response for each alloy ……... 51

Table 4.3 - Percent elongation of naturally aged specimens……. 65

Table 4.4 - Primary factors affecting ultimate tensile strength ……. 68

Table 4.5 - Average ASTM Grain Sizes of Select Samples …….. 72

LIST OF FIGURES

Figure 2.1 - Typical heating cycle for precipitation hardening treatments …… 15

Figure 2.2 - Precipitates impeding the motion of dislocations from the approach to escape (a) to (d) ……. 16

Figure 2.3. The increase in strength as precipitation progress …….. 20

Figure 3.1 - Schematic diagram of the tensile sample ……... 34

Figure 3.2 - Response and factor inputs in JMP 8 ……. 35

Figure 3.3 - The data table generated in JMP 8 ……. 36

Figure 3.4 - The fit model dialog in JMP 8 ……... 37

Figure 3.5 - The final output dialog in JMP 8 ……... 38

Figure 4.1 – Stress-strain curve for selected as-quenched samples ……... 42

Figure 4.2 - Change in hardness during one week of natural aging …….. 43

Figure 4.3 - Mean yield strength of alloys for various levels of cold work …….. 48

Figure 4.4 - Mean yield strength of alloys with and without artificial aging …… 50

Figure 4.5 - Mean yield strength of alloys with and without natural aging ……... 52

Figure 4.6 - The interaction between magnesium content and natural aging …… 54

Figure 4.7 - The effect of prior natural aging on the paint bake response ……. 55

Figure 4.8 - Yield strength variation for as-quenched alloys with various levels of silicon …….. 56

Figure 4.9 - The interaction between magnesium and silicon content for as-quenched specimens …….. 57

Figure 4.10 - The interaction between magnesium and silicon content for naturally and artificially aged specimens …….. 58

Figure 4.11 - The interaction between magnesium and copper content for naturally and artificially aged specimens …….. 59

Figure 4.12 - The interaction between silicon and copper content for naturally and artificially aged specimens …….. 61

Figure 4.13 - The effect of copper content on the paint bake strength with and without natural aging …….. 62

Figure 4.14 - The paint bake response after natural aging with and without cold working …….. 63

Figure 4.15 - Variation of ultimate tensile stress ……... 66

Figure 4.16 - Comparison of predicted and ultimate tensile strengths for naturally aged samples ……... 67

Figure 4.17 - Micrographs of selected samples. (a) OEO paint baked; and (b) OEM 10% strain + paint baked ……. 73

Figure 4.18 - Micrographs of selected samples. (a) OEH naturally aged + paint baked; and (b) OEK 10% strain + naturally aged + paint baked ……... 74

LIST OF ABBREVIATIONS AND SYMBOLS

CAFE	Corporate Average Fuel Economy
mpg	Miles travelled per gallon of fuel consumed
L/100 km	Liters of fuel consumed for every 100 kilometers travelled
σ_y	Yield strength
σ_0	Initial yield strength
σ_{CW}	Yield strength due to cold work
σ_{PPT}	Yield strength due to precipitation strengthening
σ_{REC}	Recovery strength
k_y	Constant for a given alloy system
d	Average grain diameter
SSS	Supersaturated solid solution
β	Equilibrium phase (Mg_2Si) in Al-Mg-Si alloys
GP	Guinier-Preston
β′′	A transition phase in Al-Mg-Si alloys
Q	Equilibrium phase in Al-Mg-Si-(Cu) alloys
Q′	A transition phase in Al-Mg-Si-(Cu) alloys
β′	A transition phase developed from β′′ in Al-Mg-Si alloys
θ	Equilibrium phase ($CuAl_2$) in copper-containing aluminum alloys
PBC	Paint bake cycle
PBR	Paint bake response

1 INTRODUCTION

1.1 Overview

As oil prices skyrocketed in late 1973, there was a sudden desire for smaller, more fuel efficient vehicles from the consumers for the first time. The oil crisis also illustrated how dependent western nations had become on foreign sources of oil and the negative effects such reliance could have. In 1975, in an effort to curb the nation's reliance on foreign oil, the United States Congress passed the Energy Policy and Conservation Act that established the Corporate Average Fuel Economy (CAFE) program. This program would require automobile manufacturers to meet a sales-weighted average fuel economy standard for their fleet of vehicles, a doubling of the 1974 average fuel efficiency of passenger cars by 1985 (to 27.5 mpg or 8.55 L/100 km) [1, 2]. The program was initially very successful as automobile manufacturers adopted new technologies to meet the standards. However, as oil prices fell in the mid-1980s, fuel economy was no longer as important and nearly all performance improvements made were related to the overall power, speed, and acceleration of the vehicles [1]. In fact, by 2000, the average fuel economy for a passenger car was almost 7 percent lower than in 1987-1988, when fuel economy was at its peak [1].

The 2000s have seen a rapid rise in oil prices and a new concern over the emission of greenhouse gases, primarily carbon dioxide, that contribute to global climate change. Transportation plays a central role in these issues as vehicles account for nearly 67 percent of the United States oil consumption (25 percent of worldwide demand) and nearly 30 percent of the nation's total carbon dioxide emissions (over 5 percent of worldwide emissions) [1, 3-5]. Given that automobiles contribute so heavily to the nation's oil use and greenhouse gas emissions, the United States government has recently implemented the Energy Security and Independence Act of 2007 that updates the CAFE standards for the first time since 1985. The new standards will require both cars and light trucks to have a combined fuel economy of 35 mpg (~6.7 L/100 km) by the year 2020. The new standards will be attribute based, meaning the fuel economy requirements will be matched to vehicle characteristics such as curb weight, interior volume, or "footprint" – the area covered by a vehicle's wheelbase multiplied by its track width. This closes some loopholes manufacturers previously exploited to avoid meeting the old standards. Automobile manufacturers will need to adopt new technologies and methods in order to meet the stringent requirements in the updated CAFE standards.

The average fuel economy of today's light duty vehicles is currently around 25 mpg (~9.4 L/100 km) [5, 6]. This means significant improvements need to be made if automobile manufacturers hope to achieve the goal of 35 mpg by 2020. It is estimated that only 12 to 20 percent of the original energy contained in the fuel is actually used to propel the vehicle, the remainder is lost to friction, heat loss in the exhaust and coolant, idling, and operating vehicle accessories (e.g., air conditioning) [1]. This

propulsion energy is used to overcome the inertial load of the vehicle, air resistance (aerodynamic drag), and the rolling resistance of the tires on the road. As such, there are two general ways to reduce the amount of fuel burned: (1) increase the overall efficiency of the powertrain (engine, transmission, final drive mechanism); or (2) reduce the work required to move the vehicle (weight, aerodynamics, rolling resistance, accessory load). Technologies responsible for improved fuel economy such as fuel injection, front wheel drive, improved engine aspiration (e.g., multi-valve cylinders, turbo- and super-charging), transmission technologies, improved aerodynamics, and tires with reduced rolling resistance are all reaching their technical limits. New options such as hybrid-electric, fully electric, or fuel cell vehicles face significant hurdles in further technological advancements, cost, and infrastructure requirements. It is estimated that over 80 percent of the work required to move the vehicle during city driving conditions is related to the inertia and rolling resistance of the vehicle, both of which are directly related to overall weight [1]. Thus, weight reduction offers the most significant opportunity for the reduction of fuel consumption.

1.2 Vehicle Weight Reduction

There are three primary ways to reduce the overall weight of a vehicle: (1) reduce its size; (2) optimize its design to minimize weight; and (3) substitute the materials currently used with lightweight alternatives. The first option requires a shift from larger and heavier vehicles to smaller, more lightweight options. Optimizing the design includes reducing the size of the engine and other components as vehicle

weight decreases, as well as improving the packaging of components to reduce the overall vehicle size without compromising the interior space. These options can require the consumer to go against their current wishes for large interior volumes, improved safety, and enhanced amenities such as power folding and heated seats, navigation systems, et cetera. All of these enhanced features increase the overall vehicle weight. If drastic weight reductions are to be achieved, it will require a radical increase in the use of lightweight materials.

An analysis of the mass distribution in a passenger car shows that the body is the single heaviest group, accounting for almost 45 percent of the vehicle mass; the powertrain and chassis follow with 28 and 27 percent, respectively [7]. Ferrous alloys account for over 60 percent of this mass [5, 7]. Until recently, automobile manufacturers have been reluctant to adopt new materials and manufacturing processes because of the established infrastructure, capital equipment, and also the limited knowledge base and cost of substituting with alternative lightweight materials. However, the new fuel economy, recycling, and emissions regulations have caused automakers to intensify their weight reduction attempts.

New lightweight, high strength composite materials offer one solution from a technical standpoint, but their high cost inhibits their adoption. Aluminum, meanwhile, offers the ideal engineering solution, as its density is one-third that of steel and it also satisfies the torsion and stiffness requirements of an automotive material. The mass of a vehicle's body can be reduced by almost 50 percent by simply replacing the traditional steel sheets with an aluminum alternative. When

combined with secondary weight savings opportunities, this can result in a 20-45 percent total vehicle weight reduction [5-10]. These savings are significant in terms of improving fuel economy as it is estimated that for every 10 percent weight reduction from the average new vehicle's weight, its fuel consumption will be reduced by 5-10 percent [5, 6, 8].

Aluminum also benefits from being highly recyclable. That is, the energy required for recycling aluminum is much less than the energy required for virgin production. Currently, over 60 percent of the aluminum used in producing new automobiles comes from recycled aluminum, and nearly 90 percent of aluminum contained in retired automobiles is recovered and recycled. As a result, when recycled aluminum is used, the energy per pound is comparable to that of steel, and the energy per part is actually lower [7, 11]. All of this has helped aluminum alloys become the superior choice for automotive body panels.

The main requirements for aluminum sheets that are going to be used for automotive panels have been summarized by Brünger *et al.* [10]:

(i) sufficient strength for structural stability and durability, dent resistance, and crash worthiness;

(ii) good formability for stretching, hemming, bending, and deep drawing operations in order to be competitive to automotive steel sheet;

(iii) compatibility with assembly operations (e.g., clinching, self-piercing rivets, spot welding, adhesive bonding);

(iv) excellent surface appearance after forming of final automotive parts;

(v) good corrosion resistance against filiform, stress-induced, and contact corrosion;

(vi) recyclability.

In order to meet these requirements, two types of aluminum alloys are being used commercially, namely: (i) non-heat treatable Al-Mg alloys of the 5xxx series, and (ii) heat treatable Al-Mg-Si alloys of the 6xxx series. The Al-Mg alloys are known for having very good formability, however, their final strength is relatively low compared to other aluminum alloy systems and they have a tendency to form poor surface finishes. As a result, they are primarily used for structural applications, which are not seen and often have more stringent formability requirements.

The ability of the Al-Mg-Si alloys to be formed in a relatively weak state and then to be strengthened through a heat treatment process has led to their adoption as the alloys of choice for sheet applications. Current Al-Mg-Si alloys commonly used for autobody sheet are AA6009, AA6010, AA6016, and AA6111 [10, 12]. In North America, the copper-containing alloy AA6111 is most commonly used for outer panels in gauges of 0.9-1.0 mm-thick. It develops high strength after heat treatment and has good formability [13]. Due to its relatively high copper content, AA6111 shows some susceptibility to filiform corrosion. In Europe, the cooper-free alloy AA6016 is predominantly used in gauges around 1.0-1.2 mm. It offers greater formability and corrosion resistance than AA6111, but its final strength is significantly lower. The ideal alloy would offer both excellent formability, like AA6016, and high final strength after heat treatment similar to AA6111. Such alloys

would allow for sheet thicknesses to decrease while maintaining acceptable dent resistance (providing stiffness requirements are met) thereby creating even further overall vehicle weight reductions.

1.3 Problem Definition

The formability of the Al-Mg-Si alloys is determined by numerous factors, including their chemical composition, grain size and distribution, the morphology and sizes of intermetallic particles, and the capacity of the alloy for strain hardening. The final in-service strength of the manufactured parts is only obtained after the forming operations through artificial aging, which occurs during the final automotive paint baking process. However, the natural aging that occurs between the solution heat treatment and forming, as well as the short duration of artificial aging, results in the alloys being in a heavily under-aged condition, leaving them far from the optimum strength levels that could be achieved. An ideal alloy to be used in autobody applications should thus exhibit good formability and low strength during the forming stages, and then be able to significantly strengthen during the paint bake. In order to develop such an alloy, the effect each of the various factors has on the final properties must be known. The most important factor is the chemical composition of the particular alloy, as all other factors will be influenced by it.

1.4 Research Objective

Aluminum alloys of the Al-Mg-Si series show great promise for use as outer automotive panels. The studies performed on the typical alloys used focus mostly on the strength increase due to the paint bake treatment and methods of improving it. Although a few examine the effect composition has, most only look at one specific element. While there is a good understanding of how each main solute addition contributes to the final strength of an alloy, little is reported in the open literature on the interaction effects of solutes on not only the final strength of the alloy, but also on the aging response. Therefore, the objective of this work was to investigate the combined effects the solute concentrations, natural and artificial aging, and cold working have on the final strength of a proprietary copper-containing Al-Mg-Si alloy.

1.5 Thesis Outline

This thesis has been divided into five chapters. The current chapter gives an introduction and background to the thesis topic. Chapter 2 looks at the existing work in the open literature that is relevant to the thesis topic. The experimental methods used in this study are presented in Chapter 3 and the results obtained are presented and discussed in Chapter 4. Chapter 5 summarizes the findings of this investigation and outlines some recommendations for future work.

2 LITERATURE REVIEW

This chapter will introduce the existing theoretical and experimental work in open literature on the strengthening of aluminum alloys.

2.1 Strengthening in Metals

According to crystal theory [14, 15], the strength of a perfect crystal should be much higher than the strength actually measured. This discrepancy in theoretical and measured mechanical strengths is a result of the fact that above absolute zero temperatures, all crystal structures have defects [14]. These defects can be point defects, such as vacancies or impurities, line defects, also called dislocations, surface defects, or volume defects. It is these defects that are primarily responsible for the reduction in material strength from the theoretical values.

All metals and alloys contain some dislocations that were introduced during solidification and also as a result of the thermal stresses that occur during rapid cooling. Plastic deformation in a metal corresponds to the motion of large numbers of dislocations in response to an applied stress [14, 15]. During plastic deformation, the number of dislocations increases greatly. A major source of these new dislocations are existing ones, which multiply. Other sources include grain boundaries, other

internal defects (e.g., vacancies or voids), and surface irregularities that can act as stress concentrations and serve as formation sites for new dislocations. Since plastic deformation is essentially the result of the movement of dislocations, it can be said that the ability of a metal to plastically deform is directly related to the ability of the dislocations present in the material to move freely. Since the strength of a metal is defined as its resistance to plastic deformation, it follows that its strength is a function of how easily the dislocations can move. That is, restricting the motion of dislocations in a metal will create a greater resistance to plastic deformation under a given stress, thereby increasing the strength of the metal. Virtually all strengthening techniques in metals rely on this principle: restricting or hindering dislocation motion renders a material harder and stronger [15].

2.2 Strengthening in Aluminum Alloys

There are generally four strengthening mechanisms that can be applied to aluminum alloys namely, grain size reduction, strain hardening, solid solution alloying, and precipitation hardening. The total strength of the alloy is a result of the combination of each of these factors. However, some of the strength will recover due to exposure to the elevated temperatures used during precipitation heat treatments. The net effect of the strengthening components and recovery can be represented by the following equation [16].

$$\sigma_y = \sigma_0 + \sigma_{CW} + \sigma_{PPT} - \sigma_{REC} \quad \text{..... (2.1)}$$

where σ_y is the yield strength, σ_0 is the initial strength of the material after solution heat treatment, σ_{CW} is the strength component resulting from strain hardening (or cold work), σ_{PPT} is the strength component resulting from precipitation, and σ_{REC} is the component resulting from recovery. The sub-sections that follow outline these various mechanisms and their relation to the current project.

2.2.1 Grain Size Reduction

A polycrystalline metal consists of many grains that form during cooling. As the grains form independently, they are free to develop in random orientations. As a result, the neighboring grains in any particular location within a metal will typically have slightly different orientations relative to one another. The boundaries between grains are the consequence of these mismatches in crystallographic orientation. During plastic deformation, as a dislocation moves through the metal, it will eventually encounter one of these grain boundaries and attempt to move through or across it. As explained in [15], grain boundaries can act as barriers to dislocation motion (or slip) for two reasons:

1. Since the two grains are of different orientations, a dislocation passing from one grain to another will have to change its direction of motion; this becomes more difficult as the crystallographic misorientation increases.
2. The atomic disorder within a grain boundary region will result in a discontinuity of slip planes from one grain into the other.

The effect of grain size on the yield strength of a material is often described by the Hall-Petch equation [15, 16]:

$$\sigma_y = \sigma_0 + k_y d^{-\frac{1}{2}} \qquad \text{.....} \quad (2.2)$$

In this expression, σ_y is the yield strength, d is the average grain diameter, and σ_0 and k_y are constants for the given alloy, characterizing the difficulty of transmitting slip across the boundary. It follows then that a metal with finer grains (smaller diameter) will be stronger than one that has coarse grains because there will be a greater number of grain boundaries to impede dislocation motion. However, Burger *et al.* [17] have reported that the strength of the alloys in the Al-Mg-Si (6xxx) series shows little dependence on the grain size over the ranges that can be found in commercial alloys.

2.2.2 Strain Hardening

Strain hardening, also called work hardening or cold working, is the phenomenon by which a metal is strengthened as it is plastically deformed (at relatively low temperatures). As mentioned previously, as a metal is plastically deformed, existing dislocations move throughout the material and new dislocations are also created. In general, dislocations repel each other as a result of the lattice strains associated with them [15]. As the number of dislocations increases, they begin to interact with each other and other features such as grain boundaries, both of which restrict dislocation movement. The net result is that dislocation motion is hindered, thereby increasing

the resistance of the metal to plastic deformation, i.e., increasing its strength. The cost of this enhancement, however, is a loss in ductility.

2.2.3 Solid Solution Strengthening

Metals can be strengthened by introducing impurity atoms into substitutional or interstitial positions in a pure metal to form an alloy, a technique known as solid solution strengthening. Nearly all structural metals are not highly pure, instead they have impurity atoms intentionally introduced in order to improve properties such as mechanical strength and corrosion resistance. Alloys are stronger than pure metals as a result of the lattice strains imposed by the impurity atoms that have entered into solid solution on the surrounding atoms [15]. The strain fields surrounding dislocations and those around impurity atoms tend to interact with each other such that the overall strain energy is reduced. As a result, dislocation movement is restricted because the overall lattice strain would have to increase and the alloy is thus strengthened.

All commercial aluminum alloys contain some iron and silicon, as well as at least two or more additional elements intentionally added to improve properties. The most common alloying additions to aluminum include magnesium, copper, zinc, and manganese [18]. The principal additions in the 6xxx series of aluminum alloys are magnesium, silicon, and sometimes copper.

2.2.4 Precipitation Hardening

The strength of some metal alloys can be increased by the development of small, uniformly distributed particles of a second phase within the primary phase of the alloy. These small particles, called precipitates, are formed through phase transformations that occur during heat treatment(s). This process is sometimes referred to as age hardening, or aging, because the strength increases as time passes, or as the alloy 'ages'. In order for precipitation hardening to occur, the solute (alloying additions) must have an appreciable maximum solubility in the solvent (base metal), that solubility should rapidly decrease as the temperature is reduced, and there must be lattice strains introduced at the precipitate-matrix interface [15]. In the case of aluminum alloys, only the Al-Cu (2xxx), Al-Mg-Si (6xxx), and Al-Zn (7xxx) alloy systems can be strengthened through precipitation hardening.

Precipitation hardening is achieved through two heat treatments: a solution heat treatment, followed by a precipitation heat treatment. Figure 2.1 shows a time-temperature plot of the typical heating cycle. The solution heat treatment consists of heating the alloy to a temperature, T_0, at which the solute solubility limit is sufficiently high enough to allow all of the solute atoms to be dissolved to form a single-phase solid solution (i.e., above the solvus). After the alloy has been held at the elevated temperature long enough to ensure the solute atoms are completely

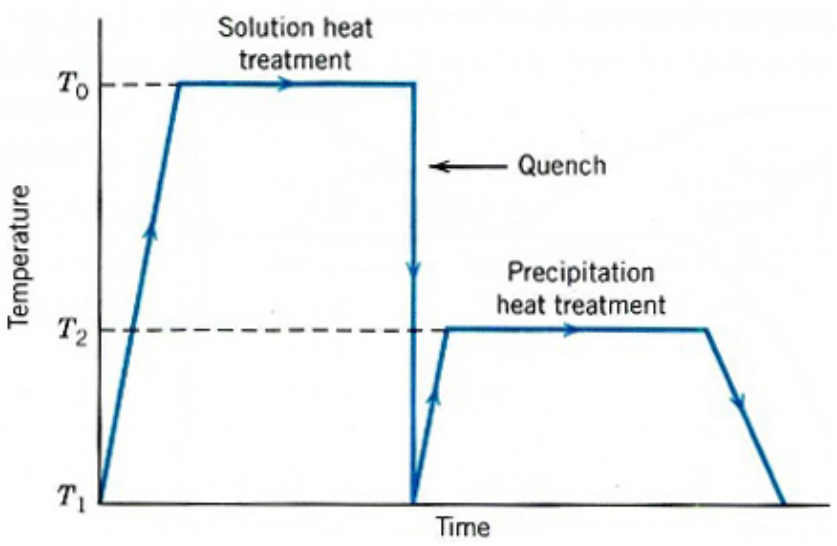

Figure 2.1. Typical heating cycle for precipitation hardening treatments. [Adapted from Callister Jr. [15]]

dissolved, it is rapidly quenched to a temperature sufficiently below the solvus such that the diffusion of any solute atoms is prevented, T_1. Thus, a non-equilibrium state exists in which the single-phase solution has become super-saturated with solute atoms that have been prevented from forming a new (secondary) phase. In the precipitation heat treatment, the supersaturated solid solution (SSS) is heated and held at an intermediate temperature below the solvus, T_2. At this temperature, the diffusion rate of the solute atoms becomes appreciable and new phases form as finely dispersed particles that have crystal structures different from the base metal. As these particles form, lattice strains are introduced at the particle-matrix interface. These lattice strains restrict dislocation motion during plastic deformation and the alloy is thus strengthened. Figure 2.2 shows how precipitate particles help prevent the movement of dislocations. Alloys that undergo significant precipitation hardening at room temperature are said to age ‘naturally’, while ‘artificial’ aging occurs at elevated temperatures.

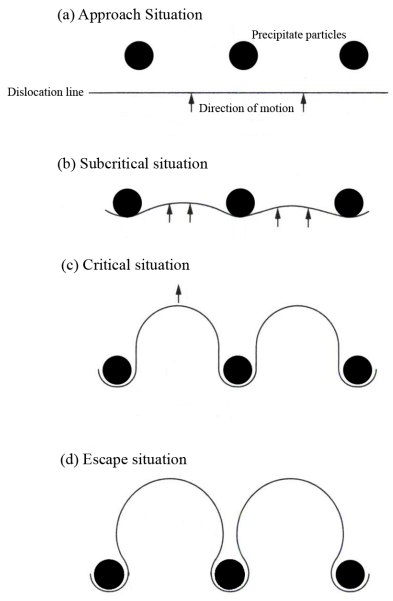

Figure 2.2. Precipitates impeding the motion of dislocations from the approach to escape, (a) to (d).

2.3 Strengthening Al-Mg-Si Alloys

The mechanical properties of aluminum alloys in the 6xxx series depend on the content of Mg, Si, Cu, and other alloying elements, treatment conditions (i.e., hot or cold working), and heat treatments. Magnesium and silicon represent the primary alloying additions and contribute to the majority of strengthening in these alloys through the precipitation of magnesium silicide (Mg_2Si), providing there is at least 0.5 wt.% of both [19]. Copper additions have also been shown to improve the strength of Al-Mg-Si alloys, however, it is usually added in limited amounts to maximize corrosion resistance (i.e., below 0.4 wt.%) . The general compositional limits of Al-Mg-Si alloys are given in Table 2.1 [18].

Table 2.1. The compositional limits for Al-Mg-Si alloys.

	Elements [wt.%]									
	Mg	Si	Cu	Ti	Cr	Mn	Fe	Ni	Zn	Zr
Maximum	1.5	1.8	1.2	0.20	0.035	1.0	1.0	0.20	2.4	0.20
Minimum	0.05	0.20	0.10	0.08	0.03	0.03	0.08	0.20	0.05	0.05

As the equilibrium Mg_2Si phase (referred to as β) develops during the precipitation heat treatment, several intermediate metastable phases are first formed as time progresses. The mechanical properties of these alloys are influenced by the nature, morphology, and amount of these intermediate particles. The sub-sections that follow will detail the precipitation sequence found in copper-containing alloys of the Al-Mg-Si system similar to those used in this study.

2.3.1 Precipitation Sequence of Al-Mg-Si-(Cu) Alloys

The precipitation response in Al-Mg-Si-(Cu) alloys is quite complex due to the presence of many intermediate phases. A great deal of research has focused on determining the sequence of precipitation events and the nature of the intermediate (and equilibrium) phases that occur in alloys of different compositions and thermomechanical histories.

In the solution treated condition, the precipitation process begins with the formation of clusters of individual magnesium atoms along with clusters of individual silicon atoms. Those clusters then give way to co-clusters of both Mg and Si. The clusters are believed to be spherical with no internal order and are so small that they are not really considered to be distinct precipitate particles [17, 20, 21]. As aging progresses, the atomic clusters develop into coherent, needle-shaped zones called Guinier-Preston (GP) zones. The preceding cluster and GP zone formation can all occur at room temperature. For further precipitation to occur, elevated temperatures are required. During artificial aging, the GP zones may either nucleate into a metastable precursor of the equilibrium Mg_2Si phase (denoted as β˝), or they may dissolve and β˝ will nucleate independently. The transition β˝ phase has a fine needle-like shape with a monoclinic structure (different lattice parameters have been reported [22-24]). At this stage of the aging process, a number of different copper-containing transition precipitates can also begin to form as well as the beginning of precipitation of Si particles. In alloys with low copper contents, a precursor to the quaternary equilibrium Q phase denoted as Q´ forms. The Q´ phase has a lath-like morphology with a hexagonal crystal structure [20, 22, 24-26] and a composition close to $Al_4Cu_2Mg_8Si_7$ [22]. In alloys containing high levels of copper, in addition to the Q´ phase, a precursor to the equilibrium $CuAl_2$ (θ) phase, denoted as θ´ also develops. During this time β˝ has transformed into semi-coherent β´ rods with a hexagonal crystal structure [17, 20, 23, 26-28]. Finally, the equilibrium phases are formed. This includes Si particles, the quaternary Q phase, and either β (Mg_2Si) or θ ($CuAl_2$) depending on the copper content. The Q phase has the same structure as Q´, but is

differentiated by its coherency with the matrix [20, 22, 24, 26]. Various compositions have been reported for the Q phase [18]. The equilibrium β phase is the stable magnesium silicide (Mg_2Si) face-centered cubic platelet [17, 20, 22, 26-29]. The equilibrium θ phase ($CuAl_2$) has a body-centered tetragonal structure [20].

The alloys under study in this project have relatively low amounts of copper, thus the precipitation sequence can be summarized as:

$$\begin{aligned} &\text{SSS} \rightarrow \text{clusters of Mg} + \text{clusters of Si atoms} \\ &\rightarrow \text{co-clusters of Mg} + \text{Si} \rightarrow \text{GP zones} \\ &\rightarrow \beta'' + \text{Q}' \rightarrow \text{equilibrium Q} + \beta\left(\text{Mg}_2\text{Si}\right) + \text{Si} \end{aligned} \qquad \ldots\ldots\ldots\ldots\ldots (2.3)$$

where SSS is the supersaturated solid solution.

The maximum strength, or peak aged condition, in Al-Mg-Si-(Cu) alloys is achieved while the precursor phases are present, prior to the formation of the equilibrium phases. It is widely reported [30] that the main strengthening phase of Al-Mg-Si-(Cu) alloys is the β´´ phase, although some Q´ may also be present in the peak aged condition. Thus the goal of most strengthening procedures is to maximize the amount of β´´ precipitates in the alloys microstructure. Figure 2.3 shows the relative increase

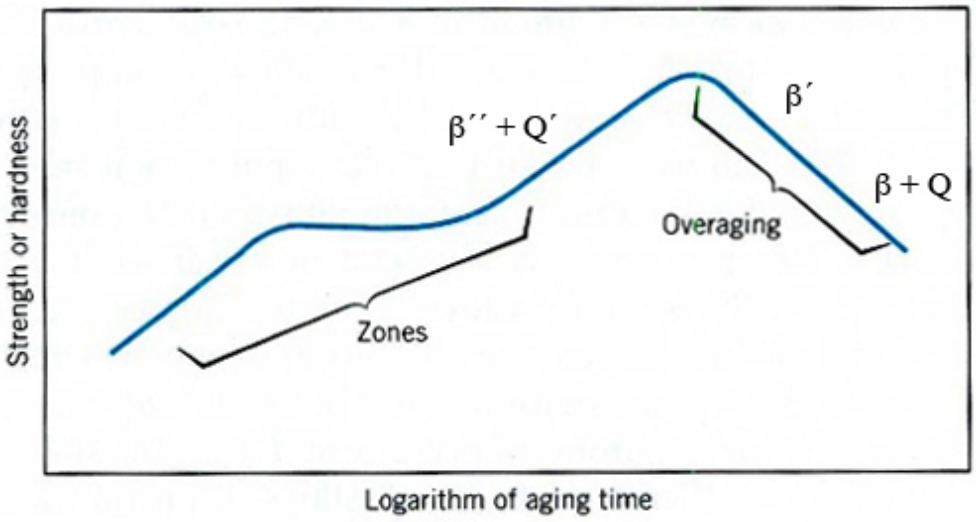

Figure 2.3. The increase in strength as precipitation progress. [Adapted from Callister Jr. [15]]

in strength with respect to time as the precipitation sequence progresses in typical aluminum alloys.

2.3.2 Natural and Artificial Aging

In the automotive industry, most aluminum sheet is supplied to the automotive manufacturers in the T4 temper [31]. That is, the sheet has been solution heat treated and allowed to stabilize at room temperature for a period of at least one week. During this period, some natural aging will occur in the alloy and atomic clusters or GP zones may be formed [30, 31]. The sheets are then formed into the required shapes prior to the assembly and final painting of the vehicle. During this final painting process the aluminum sheet is subjected to a pre-selected elevated temperature so that the paint coating(s) can be sufficiently cured to provide the desired finish. This so-called paint bake cycle (PBC) also acts as a precipitation heat treatment for the

aluminum alloys. This treatment is very important as the dent and crash resistance of the vehicle is directly related to the final strength of the alloys. To achieve peak strengthening and, therefore, the best dent/crash resistance, the β′′ phase must be formed in sufficient quantities. That can only occur during an artificial aging treatment with sufficiently high temperatures and aging times.

The automotive paint bake cycle can be approximated by aging aluminum sheet at 175-180 °C for 30 minutes [30-32]. At this temperature, the aging time is far too short for the alloys to reach their maximum strengthening potential. Various authors reported that aging to peak strength took at least six hours at 180 °C [21-24, 32]. As a result, body panels aged during the automotive paint bake cycle are always in an under aged condition [21, 22, 24, 28, 29, 33-35]. The precipitation products formed during the paint bake cycle in Al-Mg-Si-(Cu) alloys is highly dependent on the aging process and the composition of the alloy. Moons *et al.* [29] reported that only GP zones formed after artificial aging at 180 °C for 30 minutes in AA6016 alloy. Similar results were reported by Murayama *et al.* [35, 36] in copper free 6xxx series alloys. Esmaeili *et al.* [21] found that after aging at 180 °C for 30 minutes, the microstructure of AA6111 alloy contained only GP zones and some β′′. The Q′ phase that is present at peak aged conditions had not yet formed. Various authors have also reported similar findings [23, 24, 33, 37]. In a study of AA6111 alloy, Wang *et al.* [22] found that in addition to β′′, small amounts of Q′ were present after short aging times at 180 °C.

One of the most important factors affecting the type of precipitates formed during artificial aging, and thus the degree of strengthening, is the occurrence of natural aging prior to the paint bake cycle. This natural aging is inevitable in industry and nearly all studies have shown that natural aging has a negative effect on the artificial aging response of aluminum alloys [30, 32].

During natural aging, atomic clusters of magnesium and silicon precipitate and GP zones are formed [30, 31]. These precipitates are responsible for the increase in the strength of the material in the T4 temper as compared to those that have not been naturally aged. However, the increase is not very large and automotive manufacturers are interested in obtaining the largest possible strength increase, which is associated with the formation of β′′ and requires an artificial aging treatment. In order for the β′′ phase to precipitate, the clusters and zones that formed during natural aging must first be dissolved [30]. During the dissolution of these clusters and zones during the initial stages of the paint bake cycle, the strength of the material can actually decrease [20, 28]. Once sufficient dissolution has occurred, β′′ precipitation (and possibly Q′) can occur and the alloys are strengthened. Thus, the delay in β′′ precipitation caused by natural aging in combination with the relatively short duration of the paint bake cycle results in a significant reduction of the strengthening capability of the alloys. As such, there has been a focus on improving the paint bake response of aluminum alloys used for automotive body panels.

2.4 Improving the Strength of Automotive Aluminum Alloys

There are two basic methods for improving the strength of aluminum alloys used for body sheet applications. The first is to increase the initial strength of the alloy, prior to any forming or heat treatment. The second is to enhance the aging response of the alloy during any particular heat treatment. Improving the initial strength of the alloy will improve the final strength, however the increase in strength is typically coupled with a loss of formability. As a result, the sheet becomes more difficult to form – something the manufacturers want to avoid. The preferred method of improving the final strength of the alloys is to somehow improve the aging response during the automotive paint bake cycle. One of the largest contributing factors affecting the paint bake response (PBR) of an Al-Mg-Si-(Cu) alloy is its composition, in particular, the amount of silicon and the presence of copper [20, 29, 35, 38-40].

2.4.1 The Effect of Excess Silicon

Most aluminum alloys used in automotive sheet applications are said to contain excess amounts of silicon [39]. This means that there is more silicon present in the alloy than is required to form stoichiometric Mg_2Si. It is widely reported that alloys with excess silicon have higher initial strengths and a greater paint bake response compared to the balanced alloys [35, 37, 39-43]. In a balanced alloy, the ratio of magnesium to silicon atoms in the solute co-clusters, GP zones, and β´´ precipitates is close to 1.74:1. However, when excess amounts of silicon atoms are present, the

Mg:Si ratio is reduced to approximately 1:1 [24, 26, 33, 35, 36, 39]. This is very significant because the greater amount of silicon atoms can now pull more magnesium atoms out of solid solution and into strengthening precipitates. Gupta *et al.* [39] have reported that the strengthening rate and extent of strengthening increase as the amount of silicon increases until the overall Mg:Si ratio is approximately 0.4. Above that, little improvement is obtained. Table 2.2 shows the increase in T4 yield strength with increasing silicon content found by Hirth *et al*. [40].

2.4.2 The Effect of Copper

Although some solid solution strengthening occurs with the addition of copper to an Al-Mg-Si alloy, its greatest effect is on the artificial aging response. The way in which copper improves the paint bake response is multi-faceted. Some authors ascribe this to a refinement of the microstructure [20, 33, 37, 42]. It is thought that the addition of copper creates a greater supersaturation of magnesium and silicon that results in a large driving force for the creation of atomic co-clusters and GP zones during natural aging. The clusters that are formed are smaller and thus are more easily reverted during the initial stages of the paint bake cycle. As a result, there is a longer time for the strengthening precipitates (e.g., β´´) to possibly form.

The addition of copper can also change the precipitation sequence through the formation of the Q´ phase during the paint bake cycle or by decreasing the time

Table 2.2. Increasing yield strength with increasing silicon content.

Si Content [wt.%]	T4 Yield Strength [MPa]
0.81	95
0.94	104
1.06	109
1.18	116
1.39	115

needed to form the β′′ phase. It is thought copper additions greater than 0.25 wt.% are needed for this to occur [38]. Murayama *et al.* [33] and Ji *et al.* [38] have both reported that the addition of copper to an alloy caused β′′ to form when it previously had not been found. This suggests that copper-containing alloys will strengthen faster than those without any copper.

3 MATERIALS AND EXPERIMENTAL PROCEDURE

This chapter details the materials, heat treatment procedures, and the experimental techniques used during the study.

3.1 Research Plan

The goal of this research is to determine the effect the levels of magnesium, silicon, and copper have on the strength and strain aging behavior of a proprietary copper containing Al-Mg-Si aluminum alloy used for automotive sheet applications. To accomplish this goal, a full factorial experimental design was used. Using this type of design helps determine if and how a factor affects a response. It also allows for the study of the interactions between the primary factors. The study initially began as a 2^3 full factorial design with the solute concentrations of magnesium, silicon, and copper representing the main parameters. However, the effect of applied strain (cold work), natural aging, and artificial aging on these alloys was also to be studied. These parameters were also included in the study as two-level factors, resulting in a final 2^6 full factorial design. Table 3.1 shows each of the main parameters and their respective levels or values (+ represents high level, - represents low level). The full experimental design (with no repetitions) is shown in Table 3.2.

Table 3.1. The main parameters studied and their levels.

Levels	Main Factors					
	Mg	Si	Cu	Natural Aging	Artificial Aging	Applied Strain
-	0.50	0.60	0.10	No	No	0 %
+	0.80	0.90	0.30	Yes	Yes	5 %

Table 3.2. The 2^6 full factorial experimental design table.

Run	Pattern	Main Factors					
		Mg	Si	Cu	Natural Aging	Artificial Aging	Applied Strain
1	--- ---	0.5	0.6	0.1	No	No	0 %
2	--+ ---	0.5	0.6	0.3	No	No	0 %
3	-+- ---	0.5	0.9	0.1	No	No	0 %
4	-++ ---	0.5	0.9	0.3	No	No	0 %
5	+-- ---	0.8	0.6	0.1	No	No	0 %
6	+-+ ---	0.8	0.6	0.3	No	No	0 %
7	++- ---	0.8	0.9	0.1	No	No	0 %
8	+++ ---	0.8	0.9	0.3	No	No	0 %
9	--- +--	0.5	0.6	0.1	Yes	No	0 %
10	--+ +--	0.5	0.6	0.3	Yes	No	0 %
11	-+- +--	0.5	0.9	0.1	Yes	No	0 %
12	-++ +--	0.5	0.9	0.3	Yes	No	0 %
13	+-- +--	0.8	0.6	0.1	Yes	No	0 %
14	+-+ +--	0.8	0.6	0.3	Yes	No	0 %
15	++- +--	0.8	0.9	0.1	Yes	No	0 %
16	+++ +--	0.8	0.9	0.3	Yes	No	0 %
17	--- -+-	0.5	0.6	0.1	No	Yes	0 %
18	--+ -+-	0.5	0.6	0.3	No	Yes	0 %
19	-+- -+-	0.5	0.9	0.1	No	Yes	0 %
20	-++ -+-	0.5	0.9	0.3	No	Yes	0 %
21	+-- -+-	0.8	0.6	0.1	No	Yes	0 %
22	+-+ -+-	0.8	0.6	0.3	No	Yes	0 %
23	++- -+-	0.8	0.9	0.1	No	Yes	0 %
24	+++ -+-	0.8	0.9	0.3	No	Yes	0 %
25	--- ++-	0.5	0.6	0.1	Yes	Yes	0 %
26	--+ ++-	0.5	0.6	0.3	Yes	Yes	0 %
27	-+- ++-	0.5	0.9	0.1	Yes	Yes	0 %
28	-++ ++-	0.5	0.9	0.3	Yes	Yes	0 %
29	+-- ++-	0.8	0.6	0.1	Yes	Yes	0 %
30	+-+ ++-	0.8	0.6	0.3	Yes	Yes	0 %

Run	Pattern	Mg	Si	Cu	Natural Aging	Artificial Aging	Applied Strain
31	++- ++-	0.8	0.9	0.1	Yes	Yes	0 %
32	+++ ++-	0.8	0.9	0.3	Yes	Yes	0 %
33	--- --+	0.5	0.6	0.1	No	No	5 %
34	--+ --+	0.5	0.6	0.3	No	No	5 %
35	-+- --+	0.5	0.9	0.1	No	No	5 %
36	-++ --+	0.5	0.9	0.3	No	No	5 %
37	+-- --+	0.8	0.6	0.1	No	No	5 %
38	+-+ --+	0.8	0.6	0.3	No	No	5 %
39	++- --+	0.8	0.9	0.1	No	No	5 %
40	+++ --+	0.8	0.9	0.3	No	No	5 %
41	--- --+	0.5	0.6	0.1	Yes	No	5 %
42	--+ --+	0.5	0.6	0.3	Yes	No	5 %
43	-+- --+	0.5	0.9	0.1	Yes	No	5 %
44	-++ --+	0.5	0.9	0.3	Yes	No	5 %
45	+-- --+	0.8	0.6	0.1	Yes	No	5 %
46	+-+ --+	0.8	0.6	0.3	Yes	No	5 %
47	++- --+	0.8	0.9	0.1	Yes	No	5 %
48	+++ --+	0.8	0.9	0.3	Yes	No	5 %
49	--- -++	0.5	0.6	0.1	No	Yes	5 %
50	--+ -++	0.5	0.6	0.3	No	Yes	5 %
51	-+- -++	0.5	0.9	0.1	No	Yes	5 %
52	-++ -++	0.5	0.9	0.3	No	Yes	5 %
53	+-- -++	0.8	0.6	0.1	No	Yes	5 %
54	+-+ -++	0.8	0.6	0.3	No	Yes	5 %
55	++- -++	0.8	0.9	0.1	No	Yes	5 %
56	+++ -++	0.8	0.9	0.3	No	Yes	5 %
57	--- +++	0.5	0.6	0.1	Yes	Yes	5 %
58	--+ +++	0.5	0.6	0.3	Yes	Yes	5 %
59	-+- +++	0.5	0.9	0.1	Yes	Yes	5 %
60	-++ +++	0.5	0.9	0.3	Yes	Yes	5 %
61	+-- +++	0.8	0.6	0.1	Yes	Yes	5 %
62	+-+ +++	0.8	0.6	0.3	Yes	Yes	5 %
63	++- +++	0.8	0.9	0.1	Yes	Yes	5 %
64	+++ +++	0.8	0.9	0.3	Yes	Yes	5 %

By using a factorial design, it is possible to determine which parameters are statistically significant and how they interact with each other (e.g., how does the amount of copper affect the artificial aging response?). In order to establish the mechanical properties and behavior of the alloys under study, characterization techniques such as mechanical testing (i.e., microhardness measurements and tensile testing) and optical microscopy (i.e., grain sizing) were used. The results obtained were analyzed using the commercial JMP 8 software package (produced by SAS) to determine the significant primary and interaction effects.

3.2 Materials

The alloys used in this study were supplied by Novelis North America, a subsidiary of Hindalco Industries Ltd., in the form of ~1 mm-thick sheet. Novelis homogenized the ingots at approximately 560 °C for eight hours, hot rolled, and then cold rolled them to the final thickness prior to shipment. The compositions, as supplied by Novelis, of each of the eight alloys studied are presented in Table 3.3. The designation system used is the same as that provided by Novelis.

Table 3.3. Chemical composition of the alloys studied.

Alloy ID	Element [wt.%]						
	Cu	Mg	Si	Fe	Mn	Ti	Al
OEH	0.10	0.51	0.61	0.21	0.15	0.018	Bal.
OEI	0.10	0.81	0.62	0.22	0.16	0.018	Bal.
OEJ	0.10	0.81	0.89	0.23	0.16	0.018	Bal.
OEK	0.10	0.50	0.91	0.22	0.15	0.018	Bal.
OEL	0.29	0.50	0.90	0.23	0.15	0.018	Bal.
OEM	0.29	0.80	0.90	0.23	0.15	0.018	Bal.
OEN	0.29	0.49	0.59	0.23	0.15	0.018	Bal.
OEO	0.29	0.80	0.61	0.24	0.15	0.017	Bal.

3.3 Experimental Procedure

In the sub-sections that follow, a discussion of the various experimental procedures and techniques used during the study is presented. It should be noted that all mechanical testing was carried out at room temperature (~22 °C).

3.3.1 Thermal Processing

The thermal processing of each sample was initiated by a solution heat treatment at 560 ± 5 °C for 30 minutes (ASTM B 918 standard for 6061). The temperature and duration ensured all the solutes had gone into solid solution. Following the heat treatment, the samples were removed from the furnace and quenched in laboratory water (~20 °C) to keep the alloys in solid solution. The samples were then subjected to various levels of strain and to different thermal treatments, that is, natural aging, artificial aging, or a combination thereof.

For the experiments involving natural aging, the samples were allowed to age at room temperature (~22 °C) for seven days after the solution heat treatment. This period of time reflects the practice used by Novelis in supplying material to manufacturers (i.e., in the T4 temper). Once the samples had been sufficiently aged, some of the specimens were given 5 percent strain in tension while others were kept unstrained. This straining served to simulate the strains encountered by the material during automotive forming operations. All of the specimens were then stabilized at room temperature for a period of 24 hours before the final testing.

For the artificial aging experiments, following the initial solution heat treatment, some samples were subjected to 5 percent strain in tension, while the remaining were left unstrained. Again, a 24 hour stabilization period followed prior to the final treatment. To simulate the paint bake procedure used in industry, all the samples were

subsequently artificially aged at 180 ± 5 °C for 30 minutes after which time they were allowed to air cool.

The final treatment examined the combined effect of natural aging prior to artificial aging. Following solution heat treatment, the samples were aged at room temperature for a period of one week. At this time some of the specimens were given 5 percent strain in tension, while the remainder were left unstrained. After a 24 hour stabilization period, all of the specimens were subjected to the simulated paint bake cycle and finally tested.

3.3.2 Mechanical Properties

Microhardness measurements and tensile testing examined the mechanical behavior of the experimental alloys as related to their thermomechanical treatment. Tensile test specimens were machined from the 1 mm-thick sheets according to the ASTM E-8 standard, with a gauge length of 50 mm and a gauge width of 12.5 mm. Figure 3.1 shows a schematic of the tensile samples used during testing. The tensile tests were conducted at room temperature on an Instron™ 5500R screw-driven universal testing machine at an initial strain rate of $1x10^{-3}$ sec^{-1}. The data were collected during the tests using the Bluehill software package incorporated with the machine. This software automatically calculated the parameters of interest, such as 0.2% offset yield strength, percentage elongation, et cetera. Microhardness samples were cut from the as-received material and then subjected to the same thermal processing detailed in section 3.3.1. These were then metallurgically polished to a 1 μm finish. Vickers

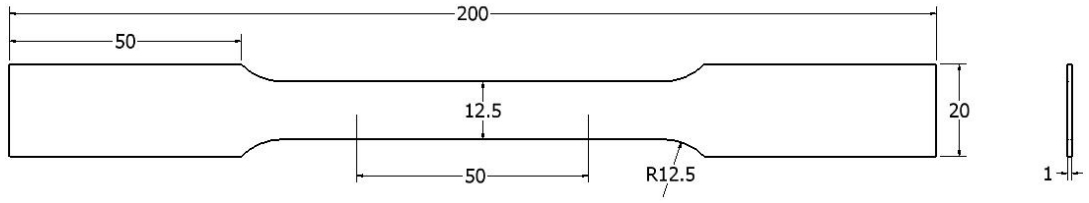

Figure 3.1. Schematic diagram of the tensile sample (all dimensions in mm).

microhardness measurements were carried out using a Mitutoyo MVK-H1 microhardness tester using a 200 g load and a dwell time of 15 seconds.

3.3.3 Statistical Model Development

The JMP 8 software package was used to create a statistical model from the full factorial experimental design to determine the significant factors affecting strength. The first stage of model development involved defining the response variable, for example, the mean yield strength. The parameters being studied and their respective values or limits are also stated. These included cold working, artificial aging, natural aging, and the amount of magnesium, silicon, and copper present. These parameters are coded as either (-) for their low level, or (+) for their high level as previously shown in Table 3.1. Figure 3.2 shows the response and factors inputs as they appear in JMP 8.

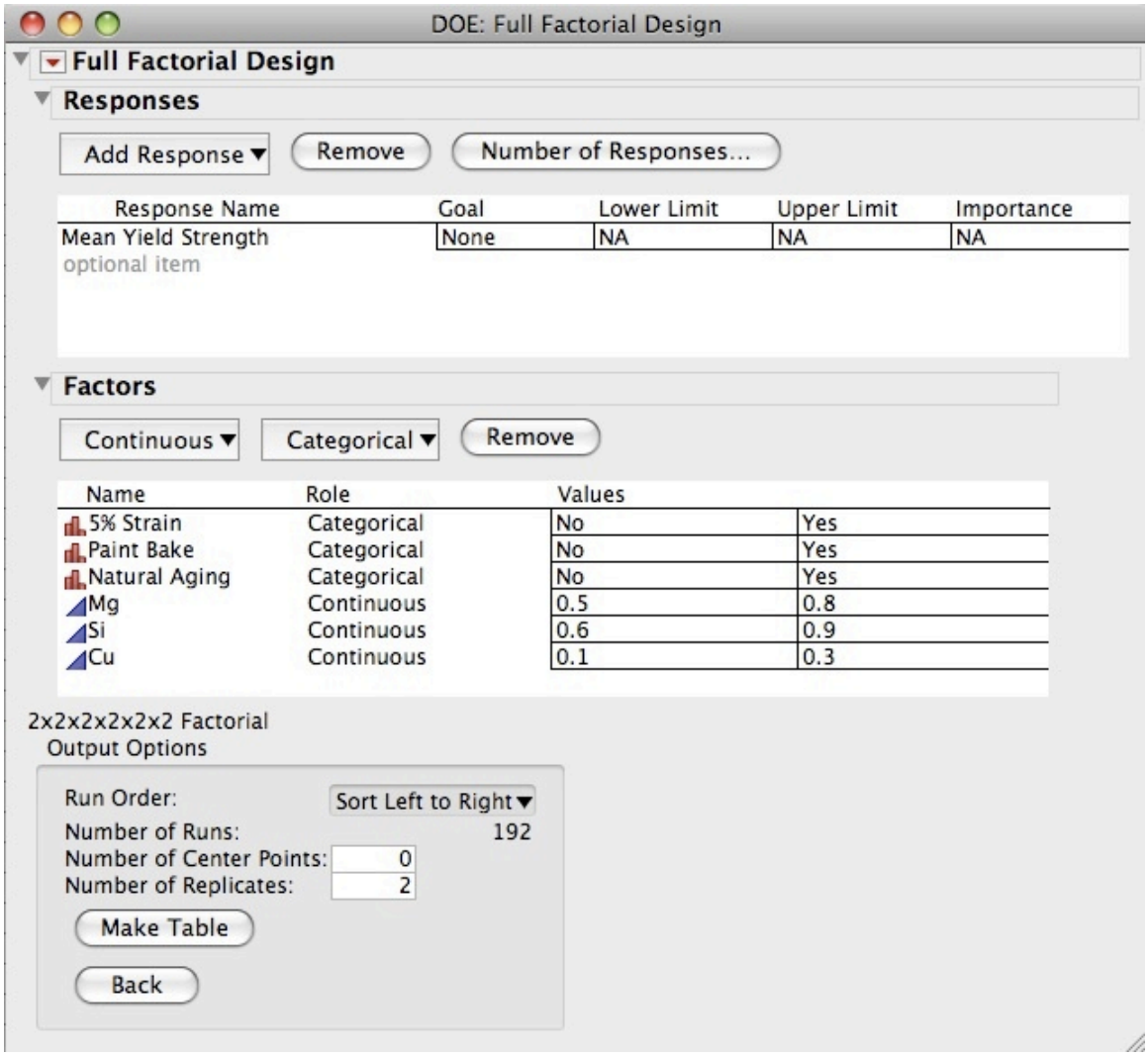

Figure 3.2. Response and factor inputs in JMP 8.

Once the response(s) and factors have been determined, JMP 8 generates a data table that displays all the experimental runs that must be completed in order to fill the model. This is essentially the experimental design table shown in Table 3.2, only the response column (e.g., mean yield strength) is empty and needs to be filled in once the results of the experiments are known. Figure 3.3 shows the data table generated for this study.

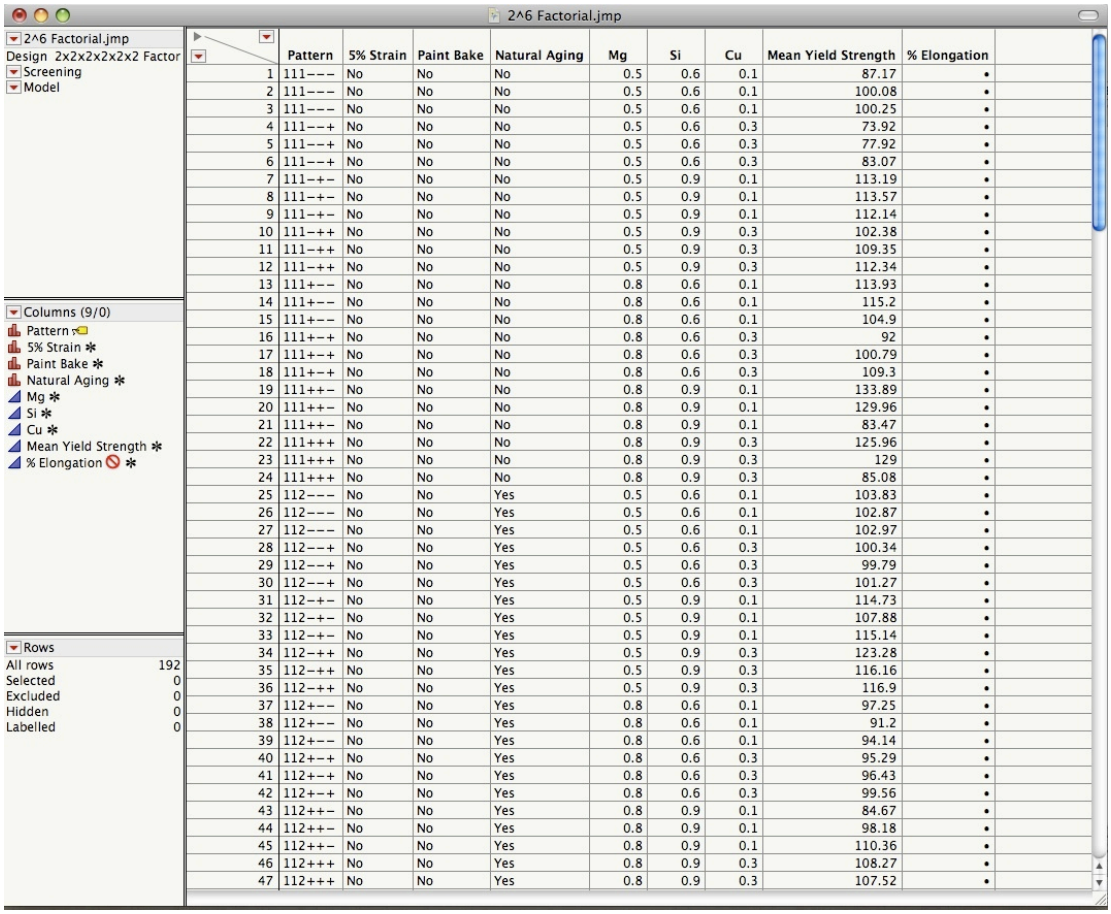

	Pattern	5% Strain	Paint Bake	Natural Aging	Mg	Si	Cu	Mean Yield Strength	% Elongation
1	111−−−	No	No	No	0.5	0.6	0.1	87.17	•
2	111−−−	No	No	No	0.5	0.6	0.1	100.08	•
3	111−−−	No	No	No	0.5	0.6	0.1	100.25	•
4	111−−+	No	No	No	0.5	0.6	0.3	73.92	•
5	111−−+	No	No	No	0.5	0.6	0.3	77.92	•
6	111−−+	No	No	No	0.5	0.6	0.3	83.07	•
7	111−+−	No	No	No	0.5	0.9	0.1	113.19	•
8	111−+−	No	No	No	0.5	0.9	0.1	113.57	•
9	111−+−	No	No	No	0.5	0.9	0.1	112.14	•
10	111−++	No	No	No	0.5	0.9	0.3	102.38	•
11	111−++	No	No	No	0.5	0.9	0.3	109.35	•
12	111−++	No	No	No	0.5	0.9	0.3	112.34	•
13	111+−−	No	No	No	0.8	0.6	0.1	113.93	•
14	111+−−	No	No	No	0.8	0.6	0.1	115.2	•
15	111+−−	No	No	No	0.8	0.6	0.1	104.9	•
16	111+−+	No	No	No	0.8	0.6	0.3	92	•
17	111+−+	No	No	No	0.8	0.6	0.3	100.79	•
18	111+−+	No	No	No	0.8	0.6	0.3	109.3	•
19	111++−	No	No	No	0.8	0.9	0.1	133.89	•
20	111++−	No	No	No	0.8	0.9	0.1	129.96	•
21	111++−	No	No	No	0.8	0.9	0.1	83.47	•
22	111+++	No	No	No	0.8	0.9	0.3	125.96	•
23	111+++	No	No	No	0.8	0.9	0.3	129	•
24	111+++	No	No	No	0.8	0.9	0.3	85.08	•
25	112−−−	No	No	Yes	0.5	0.6	0.1	103.83	•
26	112−−−	No	No	Yes	0.5	0.6	0.1	102.87	•
27	112−−−	No	No	Yes	0.5	0.6	0.1	102.97	•
28	112−−+	No	No	Yes	0.5	0.6	0.3	100.34	•
29	112−−+	No	No	Yes	0.5	0.6	0.3	99.79	•
30	112−−+	No	No	Yes	0.5	0.6	0.3	101.27	•
31	112−+−	No	No	Yes	0.5	0.9	0.1	114.73	•
32	112−+−	No	No	Yes	0.5	0.9	0.1	107.88	•
33	112−+−	No	No	Yes	0.5	0.9	0.1	115.14	•
34	112−++	No	No	Yes	0.5	0.9	0.3	123.28	•
35	112−++	No	No	Yes	0.5	0.9	0.3	116.16	•
36	112−++	No	No	Yes	0.5	0.9	0.3	116.9	•
37	112+−−	No	No	Yes	0.8	0.6	0.1	97.25	•
38	112+−−	No	No	Yes	0.8	0.6	0.1	91.2	•
39	112+−−	No	No	Yes	0.8	0.6	0.1	94.14	•
40	112+−+	No	No	Yes	0.8	0.6	0.3	95.29	•
41	112+−+	No	No	Yes	0.8	0.6	0.3	96.43	•
42	112+−+	No	No	Yes	0.8	0.6	0.3	99.56	•
43	112++−	No	No	Yes	0.8	0.9	0.1	84.67	•
44	112++−	No	No	Yes	0.8	0.9	0.1	98.18	•
45	112++−	No	No	Yes	0.8	0.9	0.1	110.36	•
46	112+++	No	No	Yes	0.8	0.9	0.3	108.27	•
47	112+++	No	No	Yes	0.8	0.9	0.3	107.52	•

Figure 3.3. The data table generated in JMP 8.

With the data table completed, the model must be fitted next. This involves describing which factors or interactions wished to be examined. In this case, a 2^6 full factorial design was used, so every possible interaction was initially examined. Figure 3.4 shows the selection of interactions in JMP 8.

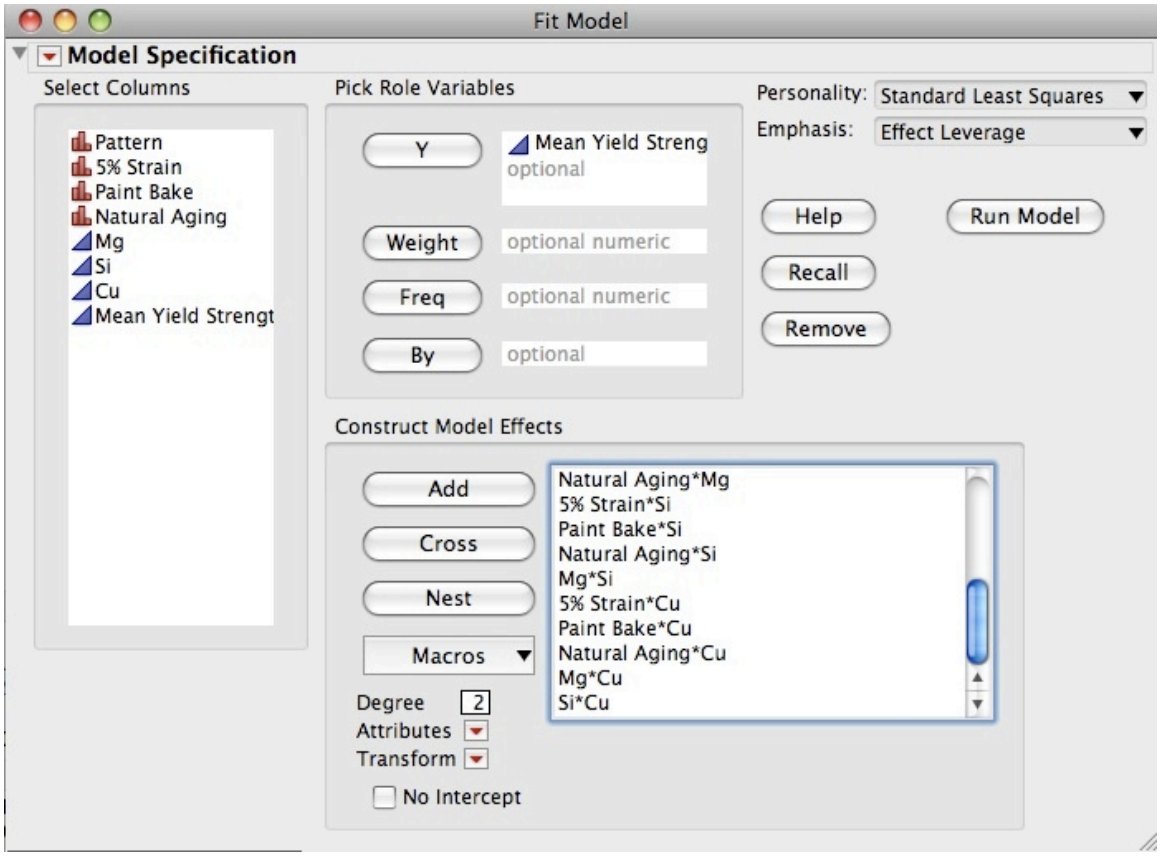

Figure 3.4. The fit model dialog in JMP 8.

Running the model will then generate the final output. This displays relevant statistical information, the significant factors and their effect, leverage plots, et cetera. Figure 3.5 shows such an output.

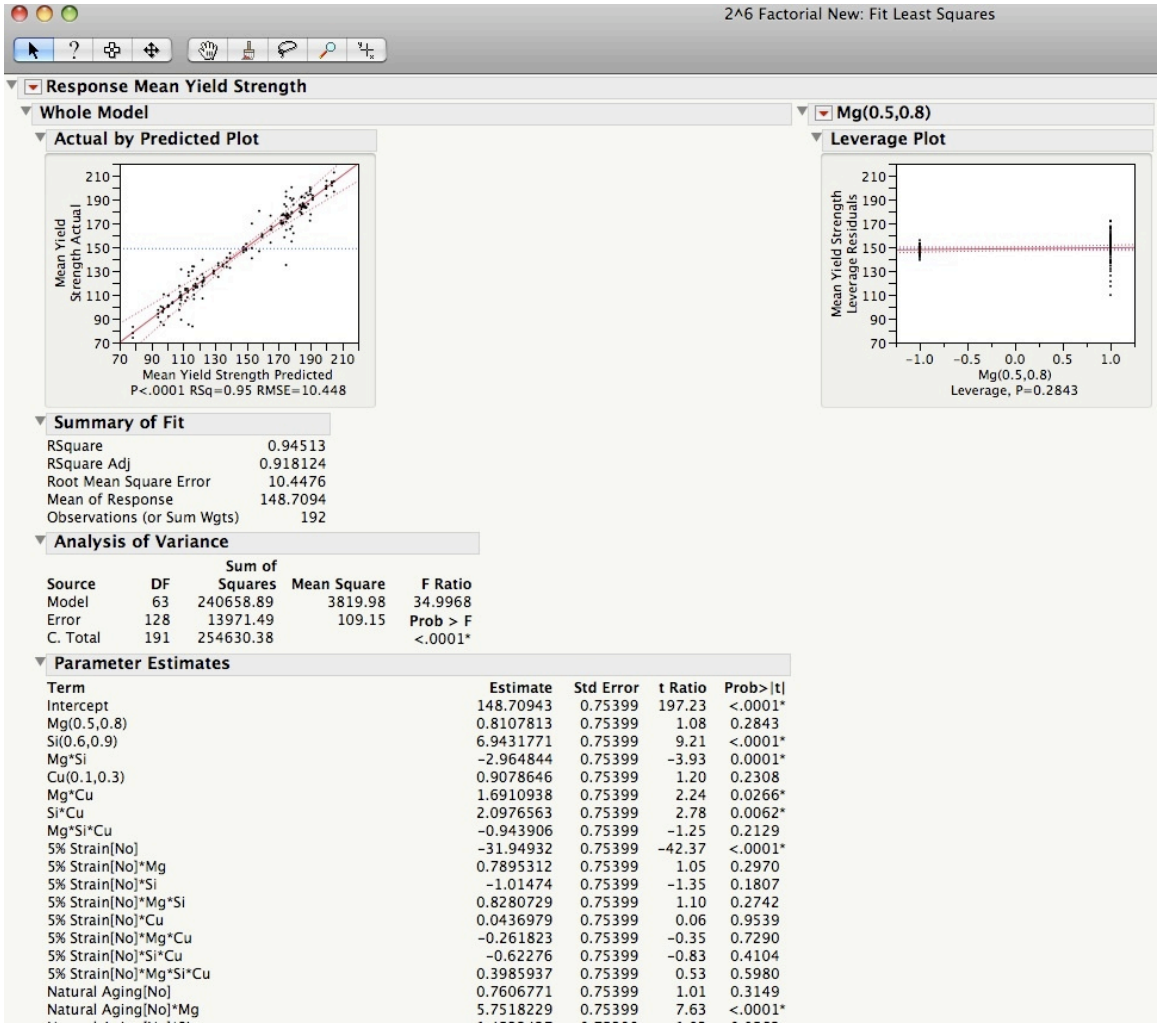

Figure 3.5. The final output dialog in JMP 8.

The effect of a particular parameter (or factor) can be determined mathematically using the following equation:

$$E_f = \overline{F}_{(+)} - \overline{F}_{(-)} \qquad \text{..... (3.1)}$$

where E_f is the effect on the response of factor f, $\overline{F}_{(+)}$ is the average response at the high level setting for that particular factor, and $\overline{F}_{(-)}$ is the average response at the low

level setting for that factor. Equation (3.1) also applies when determining the effect of an interaction between two factors. In such a case, the values of $\overline{F}_{(+ \text{ or } -)}$ now represent the average response of the interaction (e.g., $f_1 f_2$) at the high or low level.

The effect a factor or interaction has on the response may or may not be significant. JMP 8 uses an F-test to determine which factors are significant (p-value of 5 percent or less). Once the significant factors are determined from the initial run of the model, the non-significant interactions can be removed in order to simplify the resulting prediction model. The prediction model uses a regression model to illustrate the relationship between the response and the significant effects. JMP 8 produces this prediction model in the form of a prediction equation. The prediction equation is of the form:

$$y = \beta_0 + \beta_1 x_1 + \beta_2 x_2 + \cdots + \beta_{12} x_1 x_2 + \beta_{13} x_1 x_3 + \cdots + \varepsilon \quad \ldots\ldots\ldots\ldots\ldots\ldots\ldots\ldots \quad (3.2)$$

where y is the response and β_0 is the average response. The x term represents a particular parameter and is represented by either +1 or -1 depending on the level the parameter is at. The $x_1 x_2$ term refers to the interaction between parameters x_1 and x_2. $\beta_1, \beta_2 \ldots$ are the regression coefficients associated with that particular parameter. These regression coefficients are determined by dividing the estimates of effects by 2 (for a 2-level factor). The JMP 8 software package displays these coefficients in the parameter estimates table, as seen in Figure 3.5. The ε term represents the random error component.

3.3.4 Grain Sizing

An attempt was made to determine the average grain size of all the samples under study. The samples were mounted in epoxy and polished to a sub-micron finish. Weck's reagent (100 mL H_2O, 4 g $KMnO_4$, 1 g NaOH) was then used to tint the surface of the specimens, revealing the grain boundaries (refer to Appendix A for a procedure). Unfortunately, the success rate of the tinting process was only about 50 percent and not all the specimens could be studied. The other etchants tried (Barker's reagent, Keller's reagent, and NaOH) did not reveal grain boundaries in a suitable manner. Those specimens that had grain boundaries revealed were examined under an optical microscope at 100X and the grains sized with the PAX-it! image analysis software using the concentric circles method (ASTM E-112 standard). Measurements were taken from a minimum of six different sites. From these samples it was possible to determine the average grain size and the general morphology of the samples.

4 RESULTS AND DISCUSSION

In this chapter, the results of the various experiments conducted are presented and discussed. It should be noted that the error bars in the plots presented in this chapter represent the standard deviation of the three trials run for each test.

4.1 Tensile Results

Complete tensile tests were conducted for each composition and thermomechanical treatment. The stress-strain curves generated from each test can be found in Appendix B. Figure 4.1 shows the stress-strain curve for selected as-quenched samples.

The variation seen in Figure 4.1 is primarily the result of the differences in composition between the alloys. The differences will be explored further in the sections that follow.

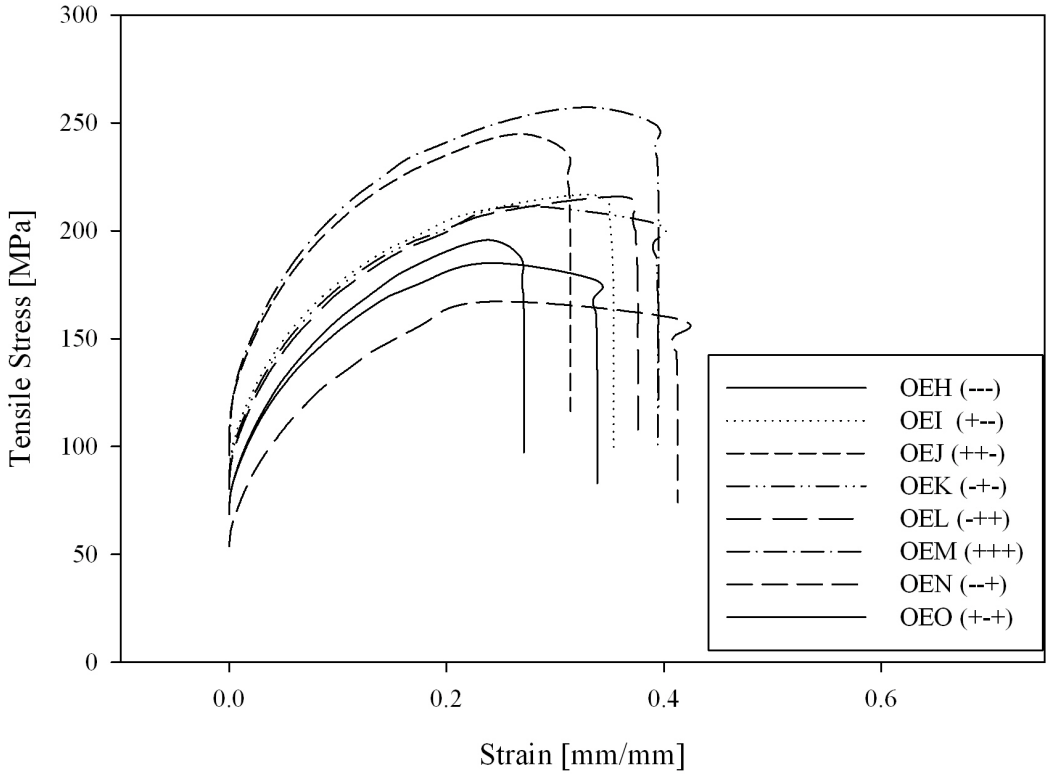

Figure 4.1. Stress-strain curve for selected as-quenched samples.

4.2 Natural Aging Behavior

A quick study of the effect that natural aging might have on the chosen alloys was carried out by monitoring the change in hardness over a one week period after the initial solution heat treatment. Figure 4.2 presents the variation of the hardness of each of the eight alloys studied with aging time. Each data point represents the average of ten hardness measurements made across the specimen. It can be observed that the greatest increase in hardening took place during the first 24 hours. After approximately 60 hours, the hardening effect slowed down greatly and remained

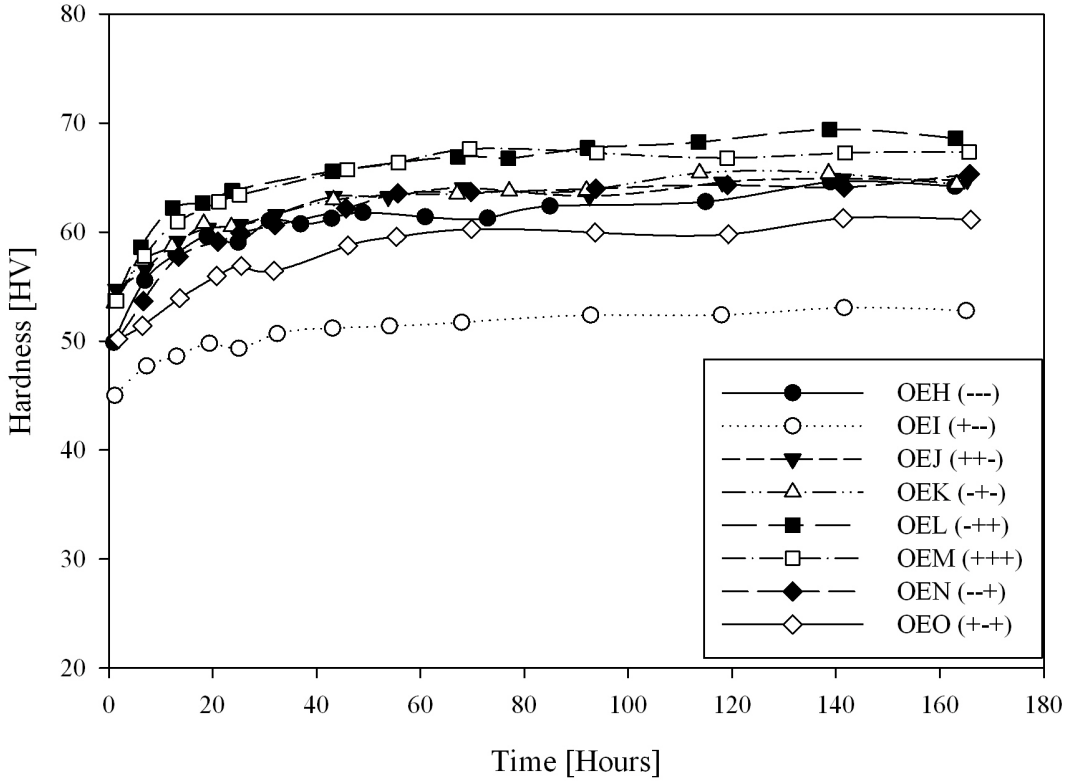

Figure 4.2. Change in hardness during one week of natural aging.

relatively constant for the remainder of the test. The average change in hardness of all the samples is 12.2 HV, which compares favorably with the results Birol [44] obtained for AA6016 alloy, although there is an appreciable difference in the chemistry of the alloys. This strengthening during natural aging suggests that some clustering took place. As such, natural aging is an important factor to consider in this study.

4.3 Main Factors Influencing the Yield Strength of the Alloys Studied

The statistical software package JMP 8 was used to examine the primary and interaction effects that a number of primary factors have on the mean yield strength of the alloys studied. The primary factors examined were the amount of magnesium, silicon, and copper in the alloys; natural aging; artificial aging (through the paint bake cycle); and cold working (5 percent strain). The least squares method was used to determine which factors and interactions had the greatest effect on the desired output, i.e., the mean yield strength. A prediction of the mean yield strength can also be made by the model. Table 4.1 lists the primary factors and interactions for the alloys studied, ranked from most significant to least. Each effect can either add to the mean yield strength, or subtract from the mean yield strength depending if it is applied or which particular level is used. This is represented with the ± symbol. Appendix C contains the table showing the statistics for each of the main factors as determined by the JMP 8 software. The prediction equation generated is given in equation (4.1).

It can be seen that the application of strain prior to the paint bake process and paint baking itself are very important, one or both being involved with over one half of the primary factors. In the sub-sections that follow, the nature of these effects will be examined.

Table 4.1. Primary factors affecting mean yield strength.

Rank	Type	Factor(s)	Effect [MPa]
1	Primary	5% Strain	± 31.95
2	Primary	Paint Bake	± 7.21
3	Primary	Si	± 6.94
4	Interaction	5% Strain * Paint Bake	± 5.24
5	Interaction	Natural Aging * Mg	± 5.75
6	Interaction	5% Strain * Natural Aging	± 3.38
7	Interaction	Paint Bake * Natural Aging	± 3.01
8	Interaction	Mg * Si	± 2.97
9	Interaction	Paint Bake * Cu	± 2.47
10	Interaction	Si * Cu	± 2.10
11	Interaction	5% Strain * Natural Aging * Mg	± 1.89
12	Interaction	Mg * Cu	± 1.69
13	Interaction	Paint Bake * Natural Aging * Cu	± 1.56

$$
\begin{aligned}
YS = {} & 148.709 \\
& + Match(\text{5\% Strain}) \begin{bmatrix} "No" \Rightarrow -31.949 \\ "Yes" \Rightarrow +31.949 \end{bmatrix} \\
& + Match(\text{Paint Bake}) \begin{bmatrix} "No" \Rightarrow -7.211 \\ "Yes" \Rightarrow +7.211 \end{bmatrix} \\
& + 6.943 * \left[\frac{(Si) - 0.75}{0.15} \right] \\
& + Match(\text{5\% Strain}) \begin{bmatrix} "No" \Rightarrow Match(\text{Paint Bake}) \begin{bmatrix} "No" \Rightarrow -5.239 \\ "Yes" \Rightarrow +5.239 \end{bmatrix} \\ "Yes" \Rightarrow Match(\text{Paint Bake}) \begin{bmatrix} "No" \Rightarrow +5.239 \\ "Yes" \Rightarrow -5.239 \end{bmatrix} \end{bmatrix} \\
& + Match(\text{5\% Strain}) \begin{bmatrix} "No" \Rightarrow Match(\text{Natural Aging}) \begin{bmatrix} "No" \Rightarrow +3.375 \\ "Yes" \Rightarrow -3.375 \end{bmatrix} \\ "Yes" \Rightarrow Match(\text{Natural Aging}) \begin{bmatrix} "No" \Rightarrow -3.375 \\ "Yes" \Rightarrow +3.375 \end{bmatrix} \end{bmatrix} \\
& + Match(\text{Paint Bake}) \begin{bmatrix} "No" \Rightarrow Match(\text{Natural Aging}) \begin{bmatrix} "No" \Rightarrow -3.008 \\ "Yes" \Rightarrow +3.008 \end{bmatrix} \\ "Yes" \Rightarrow Match(\text{Natural Aging}) \begin{bmatrix} "No" \Rightarrow +3.008 \\ "Yes" \Rightarrow -3.008 \end{bmatrix} \end{bmatrix} \qquad \ldots\ldots\ldots (4.1) \\
& + Match(\text{Natural Aging}) \begin{bmatrix} "No" \Rightarrow \left[\frac{(Mg) - 0.65}{0.15} \right] * 5.752 \\ "Yes" \Rightarrow \left[\frac{(Mg) - 0.65}{0.15} \right] * -5.752 \end{bmatrix} \\
& + \left[\frac{(Mg) - 0.65}{0.15} \right] * \left[\frac{(Si) - 0.75}{0.15} \right] * -2.965 \\
& + \left[\frac{(Mg) - 0.65}{0.15} \right] * \left[\frac{(Cu) - 0.20}{0.10} \right] * 1.691 \\
& + \left[\frac{(Si) - 0.75}{0.15} \right] * \left[\frac{(Cu) - 0.20}{0.10} \right] * 2.098
\end{aligned}
$$

*continued on the next page.

$$
\begin{aligned}
&+Match(\text{5\% Strain})\left[\begin{array}{l}
"No" \Rightarrow Match(\text{Natural Aging})\left[\begin{array}{l}
"No" \Rightarrow \left[\frac{(Mg)-0.65}{0.15}\right]*1.890 \\
"Yes" \Rightarrow \left[\frac{(Mg)-0.65}{0.15}\right]*-1.890
\end{array}\right] \\
"Yes" \Rightarrow Match(\text{Natural Aging})\left[\begin{array}{l}
"No" \Rightarrow \left[\frac{(Mg)-0.65}{0.15}\right]*-1.890 \\
"Yes" \Rightarrow \left[\frac{(Mg)-0.65}{0.15}\right]*1.890
\end{array}\right]
\end{array}\right] \\
&+Match(\text{Paint Bake})\left[\begin{array}{l}
"No" \Rightarrow \left[\frac{(Cu)-0.20}{0.10}\right]*-2.465 \\
"Yes" \Rightarrow \left[\frac{(Cu)-0.20}{0.10}\right]*2.465
\end{array}\right] \\
&+Match(\text{Paint Bake})\left[\begin{array}{l}
"No" \Rightarrow Match(\text{Natural Aging})\left[\begin{array}{l}
"No" \Rightarrow \left[\frac{(Cu)-0.20}{0.10}\right]*-1.556 \\
"Yes" \Rightarrow \left[\frac{(Cu)-0.20}{0.10}\right]*1.556
\end{array}\right] \\
"Yes" \Rightarrow Match(\text{Natural Aging})\left[\begin{array}{l}
"No" \Rightarrow \left[\frac{(Cu)-0.20}{0.10}\right]*1.556 \\
"Yes" \Rightarrow \left[\frac{(Cu)-0.20}{0.10}\right]*-1.556
\end{array}\right]
\end{array}\right]
\end{aligned}
$$

where *YS* is the predicted yield strength, and *(Mg)*, *(Si)*, and *(Cu)* represent the composition level of magnesium, silicon, and copper respectively.

4.3.1 The Effect of Cold Work

Figure 4.3 compares the mean yield strength for each alloy composition studied immediately after solutionizing (as-quenched) and after 5% strain in tension was

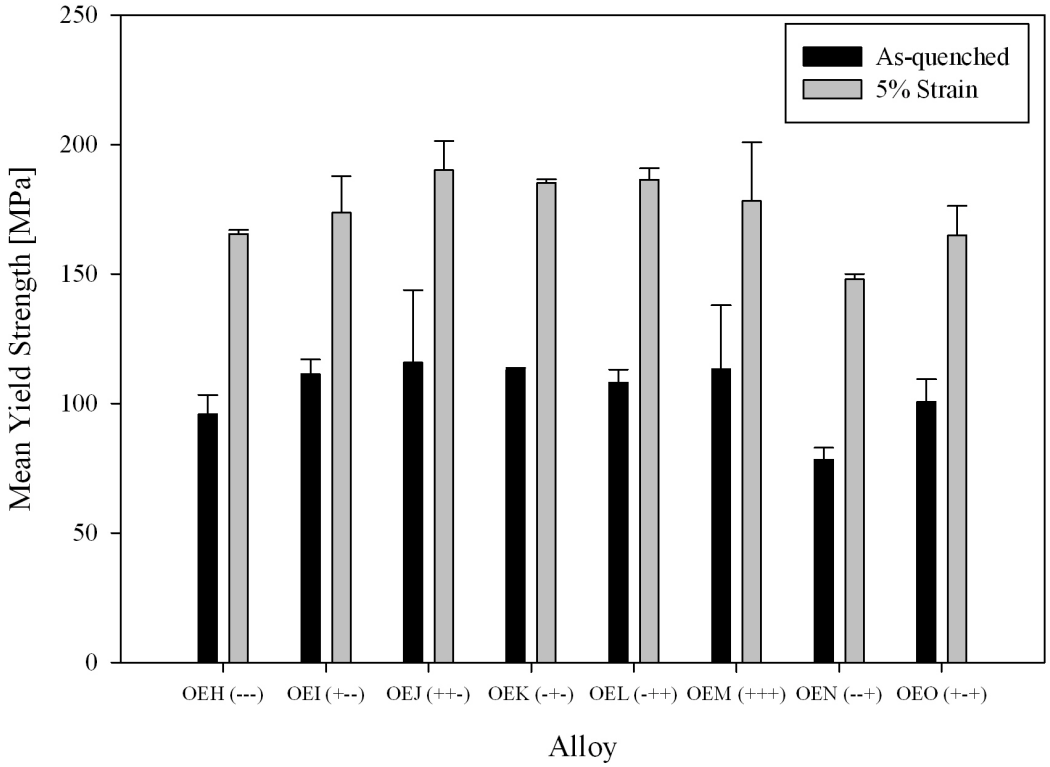

Figure 4.3. Mean yield strength of alloys for various levels of cold work.

applied. As expected, cold working prior to testing increased the mean yield strength of every alloy by approximately 70 MPa in each case. The minor differences seen between the individual alloys could be the result of compositional differences, a response to natural aging during the testing period, or simply experimental errors. For example, alloys OEH and OEN both contain low levels of magnesium and silicon (i.e., 0.5 wt.% and 0.6 wt.%, respectively) and have the lowest yield strengths of the group. The low solute levels likely produce low cluster formation which leads to the weaker strengths in the as-quenched condition.

4.3.2 The Effect of Artificial Aging During the Paint Bake Cycle

It is expected that the mean yield strength of all the alloys will increase after aging during the paint bake cycle. Figure 4.4 shows the change in the mean yield strength of the samples after aging for 30 minutes at 180 °C. This change in strength is known as the paint bake response (PBR). It can be seen that although paint baking did increase the yield strength of the alloys, the response was quite varied between the different alloys. This is most likely due to the differences in composition. Alloys OEH and OEK, which show the lowest increase in strength, all have low magnesium and copper contents (i.e., 0.5 wt.% and 0.1 wt.%, respectively). Alloys OEJ, OEM, and OEO show the highest strength levels after the paint bake treatment. Alloys OEJ and OEM both contain high levels of magnesium and silicon (i.e., 0.8 wt.% and 0.9 wt.%, respectively) which likely leads to increased precipitation during the artificial aging period. Alloy OEO contains high levels of magnesium and copper (i.e., 0.8 wt.% and 0.3 wt.%, respectively). Although silicon levels are low, the increased copper content may help improve the paint bake response. This would suggest that alloys with higher magnesium contents show a greater paint bake response, and the addition of copper improves this. This can be seen in Table 4.2 as alloys OEM and OEO, both of which contain high levels of magnesium and copper, show the greatest paint bake response. Table 4.2 also summarizes the paint bake response for each alloy.

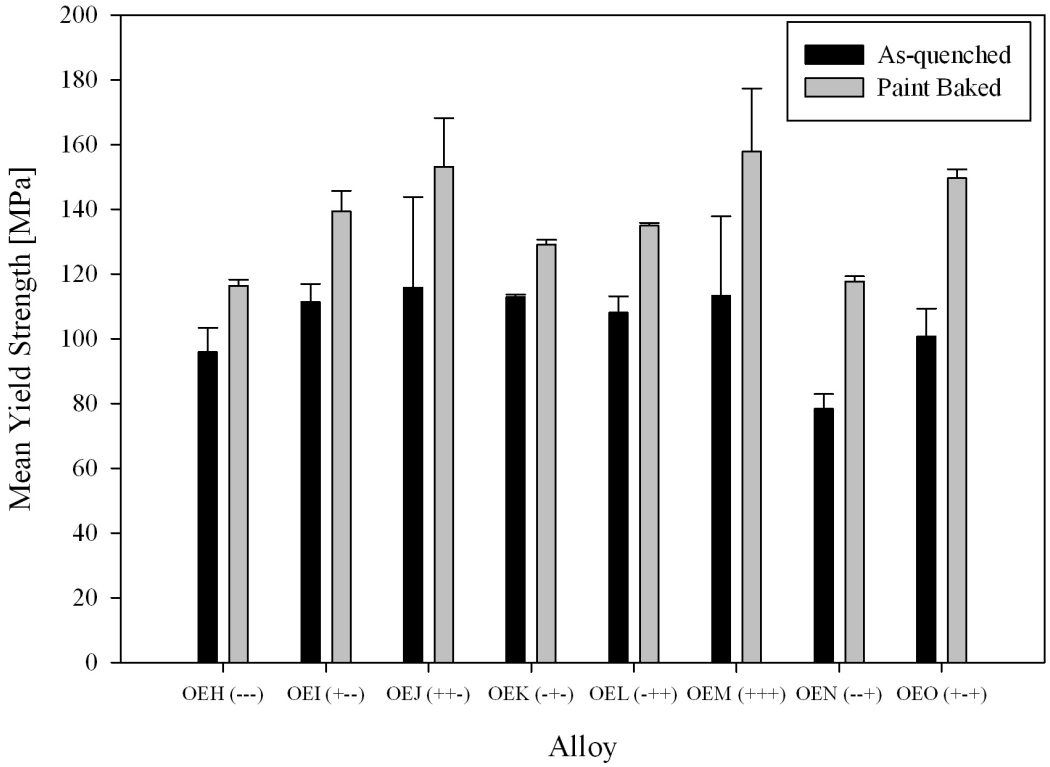

Figure 4.4. Mean yield strength of alloys with and without artificial aging.

Table 4.2. The paint bake response for each alloy.

Designation	Mean Yield Strength [MPa]		
	As-quenched	Paint Baked	PBR
OEH	95.83 ± 7.50	116.39 ± 1.89	20.56
OEI	111.34 ± 5.62	139.41 ± 6.27	28.07
OEJ	115.77 ± 28.04	153.18 ± 15.00	37.40
OEK	112.97 ± 0.74	129.13 ± 1.39	16.16
OEL	108.02 ± 5.11	134.93 ± 0.87	26.91
OEM	113.35 ± 24.53	157.77 ± 19.53	44.43
OEN	78.30 ± 4.59	117.66 ± 1.60	39.36
OEO	100.70 ± 8.65	149.58 ± 2.79	48.88

4.3.3 The Influence of Natural Aging

Although natural aging is not a primary factor on its own, it remains a very important factor for a number of reasons. Firstly, it interacts with a number of other factors to produce a considerable effect on the yield strength of the alloys. Natural aging is also practically unavoidable in the industrial setting and, as such, it is important to understand what influence it might have on the alloys tested in this study. Figure 4.5 compares the mean yield strength of the alloys in the as-quenched and the T4

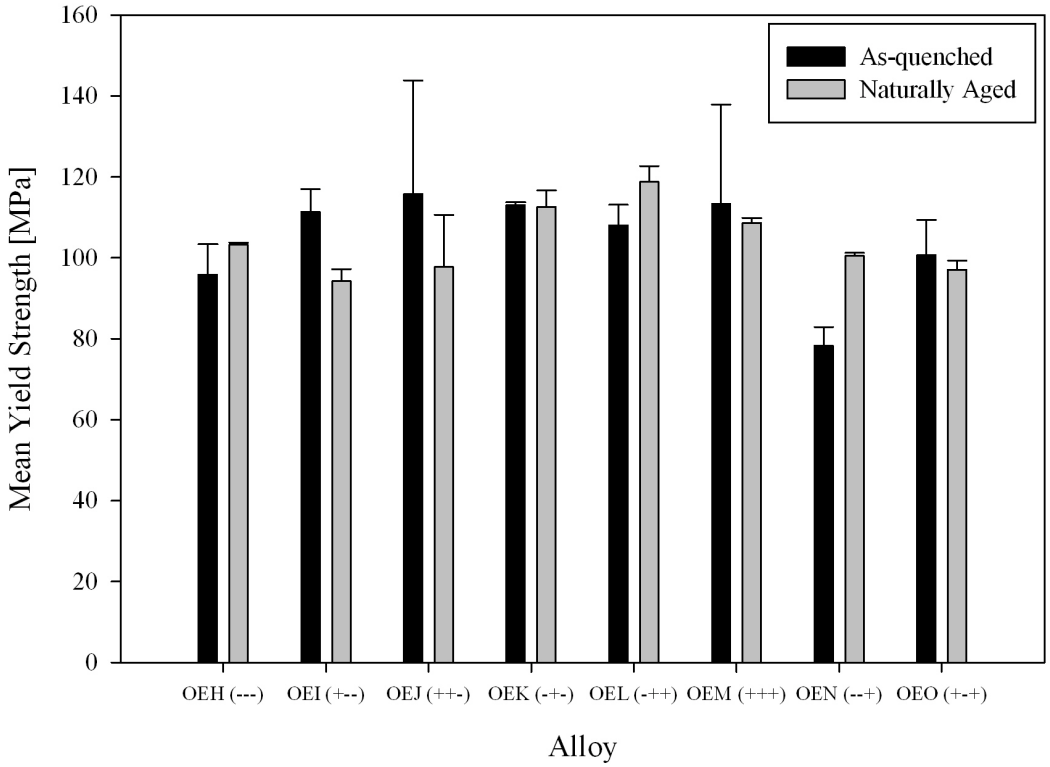

Figure 4.5. Mean yield strength of alloys with and without natural aging.

(naturally aged) condition. The average yield strength of all the naturally aged alloys is approximately 104 MPa, which compares favorably with the results Hirth *et al.* [40] found for a AA6016 alloy with a similar composition. This average falls below the maximum allowable T4 yield strength of 130 MPa as dictated by the automobile manufacturers [41, 45].

It can be seen in Figure 4.5 that only three of the alloys studied increase in strength by an appreciable amount (OEK remains virtually unchanged) with natural aging. The amount of strengthening is relatively small and in some cases the alloy was

actually weakened. It should be noted that the four alloys which show some weakening (OEI, OEJ, OEM, and OEO) are the four compositions that contain a higher amount of magnesium. This effect can be seen in the interaction plot of magnesium and natural aging in Figure 4.6. It is also interesting to note that the two alloys that show the least amount of weakening (i.e., OEM and OEO) have high levels of copper. Of the alloys that are strengthened, OEL and OEN contain high levels of copper and show a greater strengthening response. This suggests that copper has a strengthening effect on these alloys by reducing the negative impact of natural aging.

Figure 4.7 shows the effect of natural aging on the paint bake response of these alloys. Once again, it can be seen that the alloys with high levels of magnesium (i.e., OEI, OEJ, OEM, and OEO) show lower strengths than those with low levels of magnesium.

The combination of natural aging and paint baking most accurately resembles the conditions found in the automobile industry, and, as such, the alloys with the highest strength in this condition are of great interest. It can be noted that the two alloys (OEK and OEL) with the highest strength after the T4 and T6 aging treatments both feature low magnesium and high silicon levels. Silicon itself has a major influence on the yield strength.

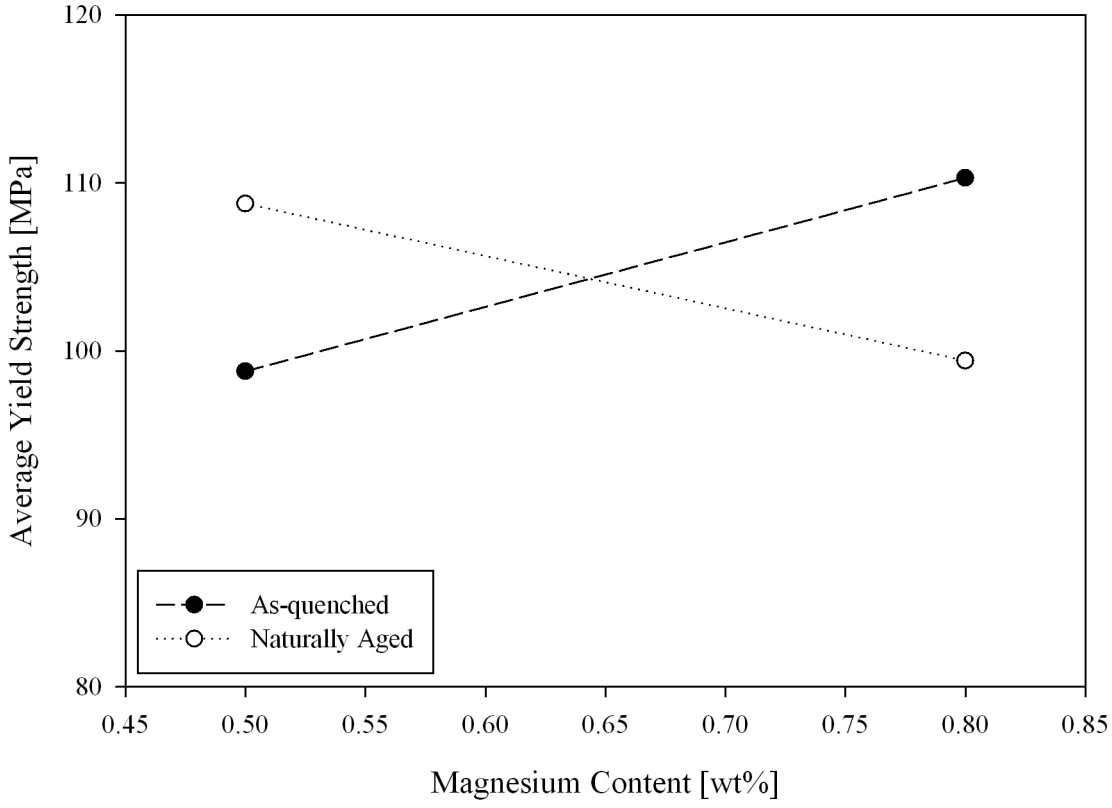

Figure 4.6. The interaction between magnesium content and natural aging.

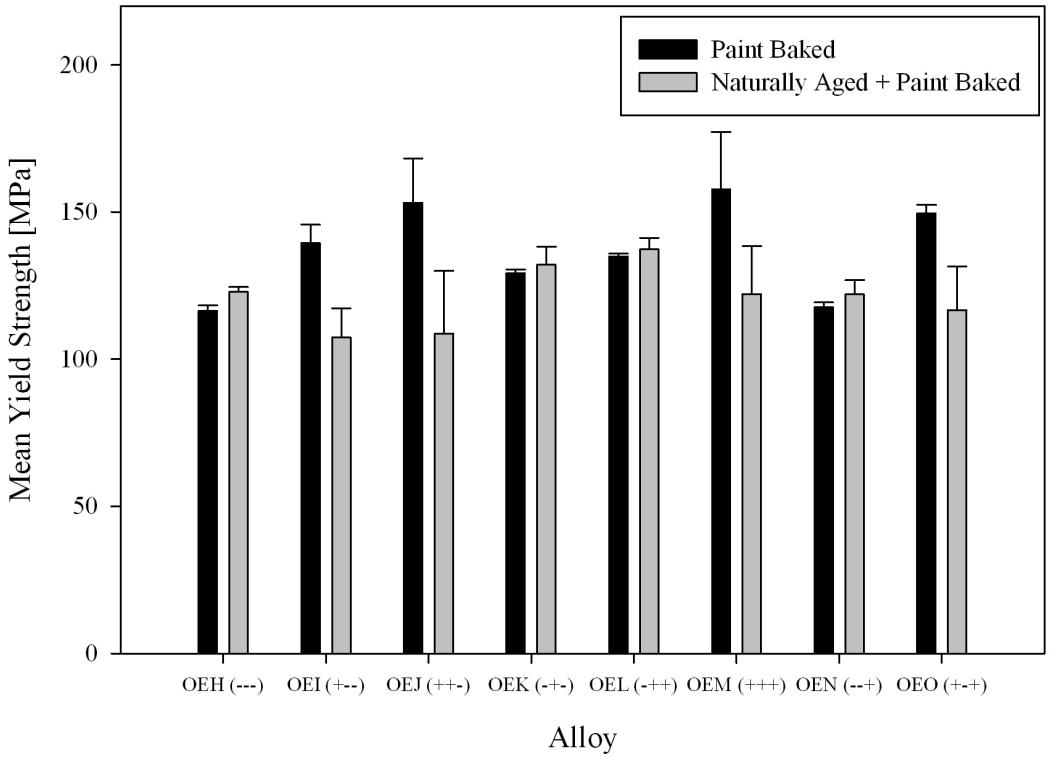

Figure 4.7. The effect of prior natural aging on the paint bake response.

4.3.4 Compositional Effects on the Yield Strength

The amount of the major alloying elements (Mg, Si, and Cu) present in the alloys can have a great effect on their yield strength. This is principally through interactions with each other (e.g., Mg and Si) and other factors such as natural and artificial aging.

Figure 4.8 shows the change in yield strength for as-quenched alloys with low and high levels of silicon (i.e., 0.6 wt.% and 0.9 wt.%, respectively). It can be seen that the alloys with higher silicon content have, on the average, higher yield strengths.

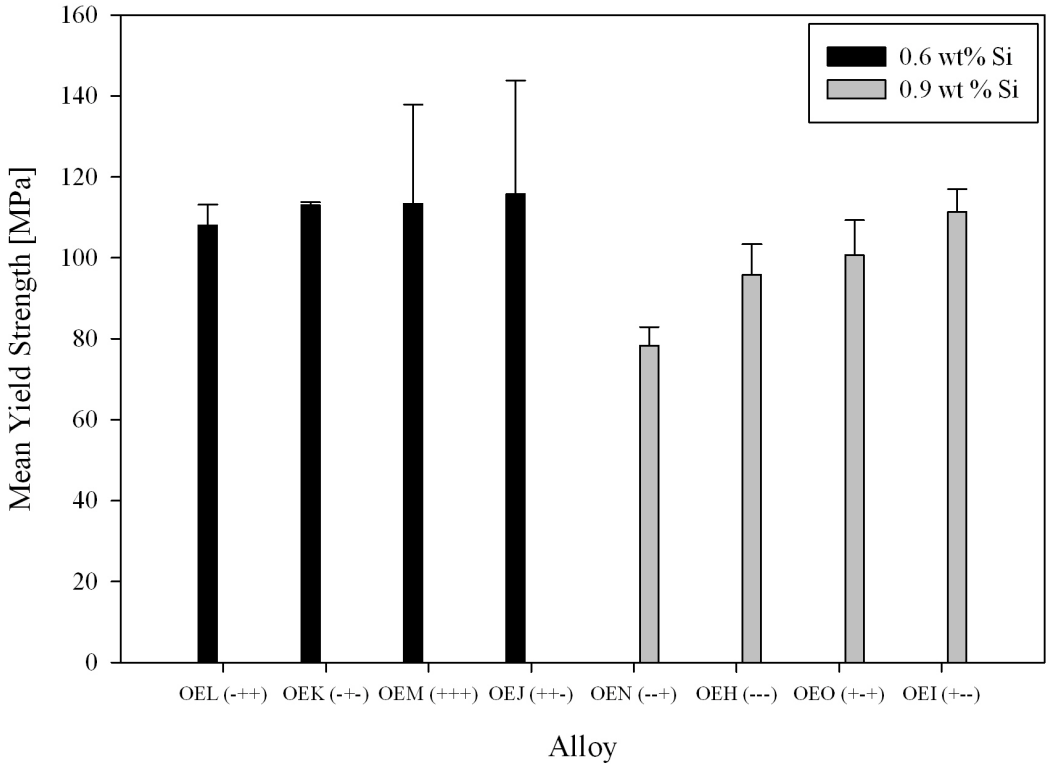

Figure 4.8. Yield strength variation for as-quenched alloys with various levels of silicon.

This agrees with previous reports that increased silicon content leads to higher strength [38, 39].

The variation present in the yield strengths shown in Figure 4.8 is most likely a result of the different compositions in each alloy. That is, different combinations of alloying element produce different strengthening levels. Figure 4.9 shows the interaction between magnesium and silicon in the as-quenched state. It can be seen that the highest strength levels occur when both magnesium and silicon are at their highest

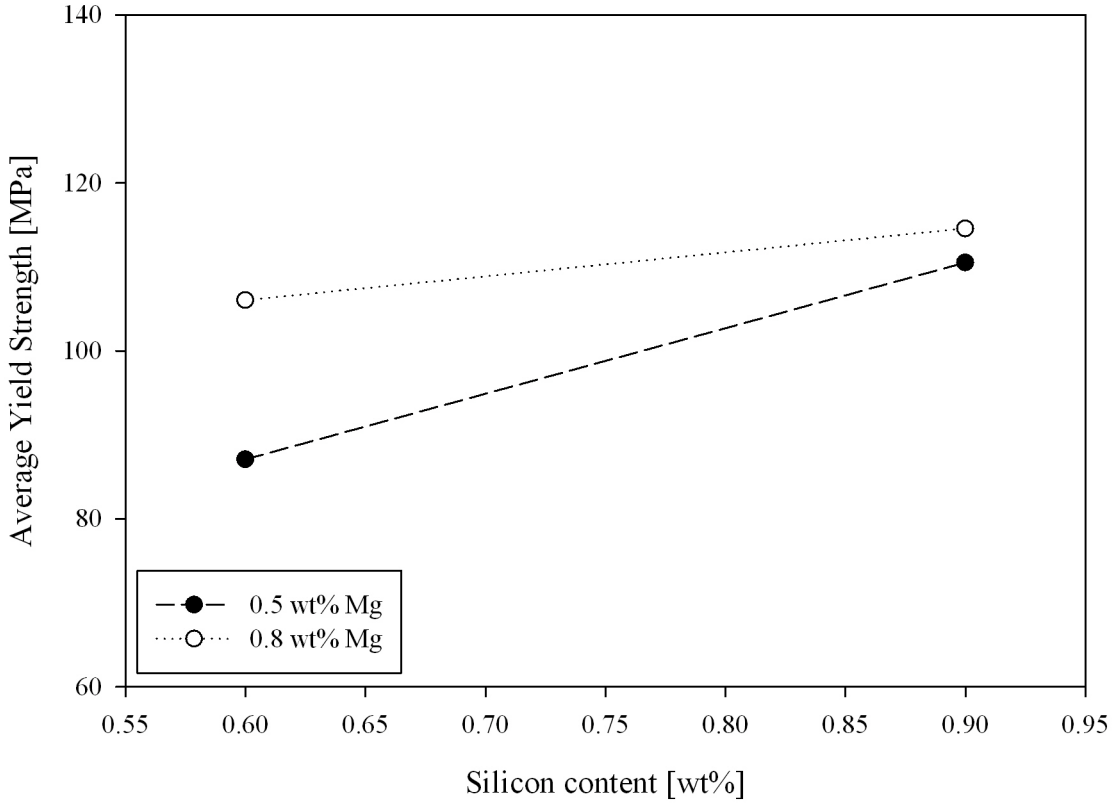

Figure 4.9. The interaction between magnesium and silicon content for as-quenched specimens.

levels. In the as-quenched state, the majority of strengthening is from solid solution strengthening and, perhaps, some early cluster formation. It follows then that more solute atoms would provide more strengthening and also a greater possibility of cluster formation.

However, the strength of the alloys in the as-quenched state is not as important as the strength after paint baking. In view of this, natural aging and the paint bake response should be accounted for. Figure 4.10 shows the interaction between magnesium and

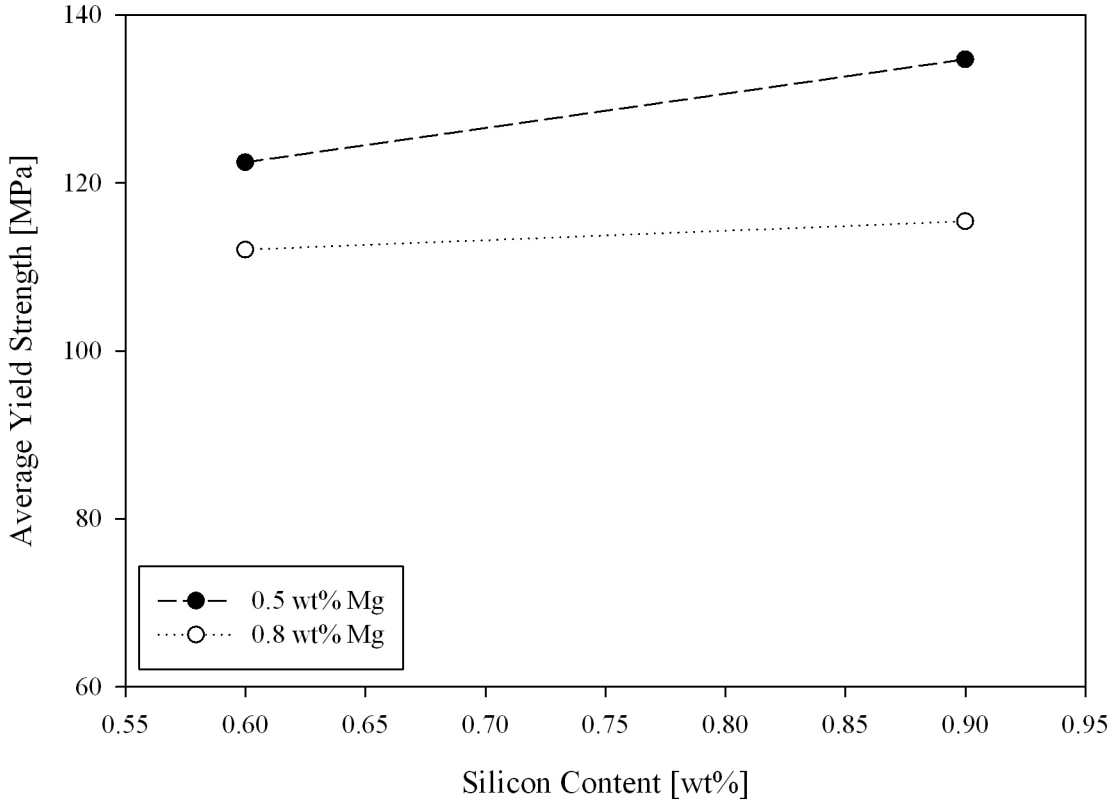

Figure 4.10. The interaction between magnesium and silicon content for naturally and artificially aged specimens.

silicon for samples subjected to a combined T4 and T6 treatment. It can be seen that higher strengths were achieved in the naturally aged and paint baked conditions when magnesium levels are low (i.e., 0.5 wt.%). Higher levels of silicon also improved the yield strength as seen in Figure 4.10.

The addition of copper to the ternary Al-Mg-Si alloys has a great effect on its properties. According to the model generated by the JMP 8 software, copper interacts with numerous factors that affect the yield strength of the alloys. Figure 4.11 shows

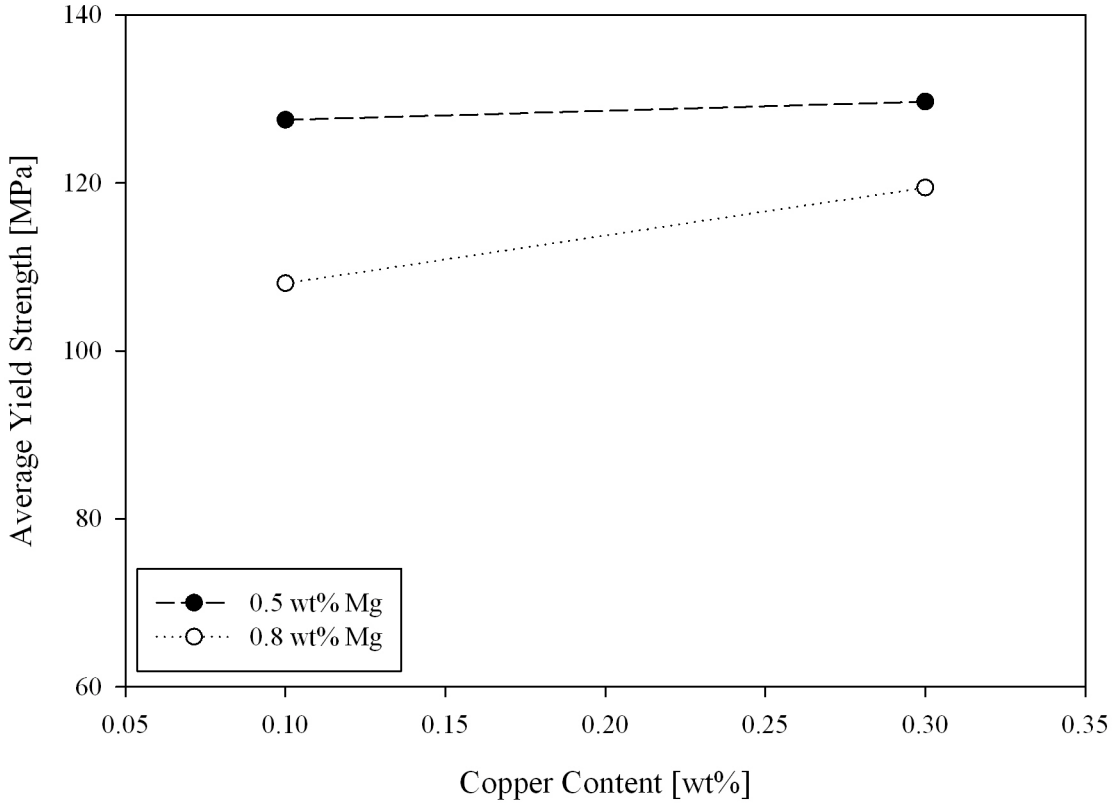

Figure 4.11. The interaction between magnesium and copper content for naturally and artificially aged specimens.

the interaction of magnesium and copper in samples subjected to T4 and T6 (paint bake) treatments. It can be seen that low levels of magnesium promote the highest average yield strength and copper has little effect at these magnesium levels. It is interesting to note however that at high levels of magnesium, copper does show an effect on the average yield strength (approximately 12 MPa). This effect could be attributed to a number of factors. As pointed out in section 4.3.3, increased levels of copper reduced the negative effect of natural aging in alloys with high levels of magnesium. Increasing the copper content could create a greater supersaturation of

magnesium and silicon in the alloys that results in higher precipitate formation, especially in those alloys with higher magnesium and silicon contents. The presence of greater amounts of copper may also enhance the formation of copper-containing precipitates during the artificial aging treatment (e.g., Q´ phase) that strengthen the alloys.

Figure 4.12 displays the interaction between silicon and copper in the samples that were naturally aged and paint baked. It can be seen that the highest average yield strength is achieved when both silicon and copper are at their highest levels. The degree of strengthening associated with an increase in copper content is greater for alloys with 0.9 wt.% silicon (approximately 9 MPa) than those with 0.6 wt.% silicon (approximately 4 MPa). Higher copper and silicon levels may create a greater supersaturation of the matrix, thereby resulting in greater precipitation of strengthening phases [46].

Copper also has an appreciable effect on the paint bake response of the alloys. Figure 4.13 shows the effect of copper on the paint baked strength of the alloys with and without natural aging. Once again, it can be seen that high levels of copper promotes high yield strengths. The negative effect of natural aging on the final strength after paint baking can also be seen.

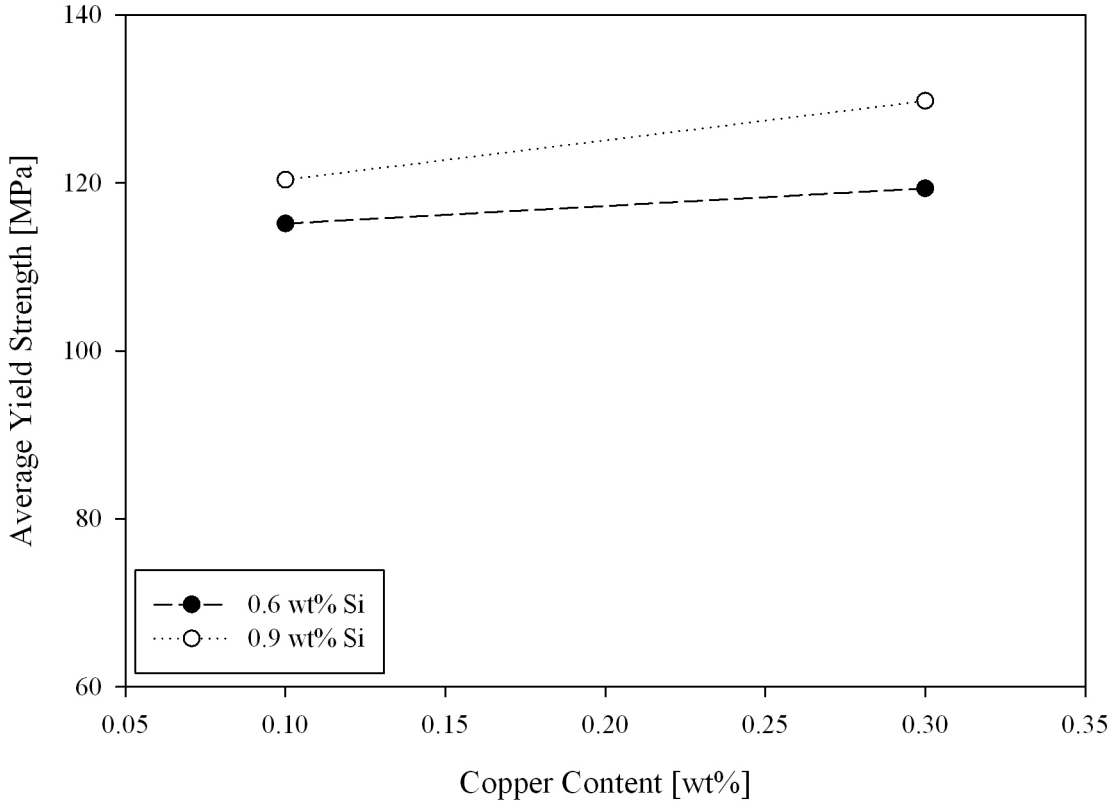

Figure 4.12. The interaction between silicon and copper content for naturally and artificially aged specimens.

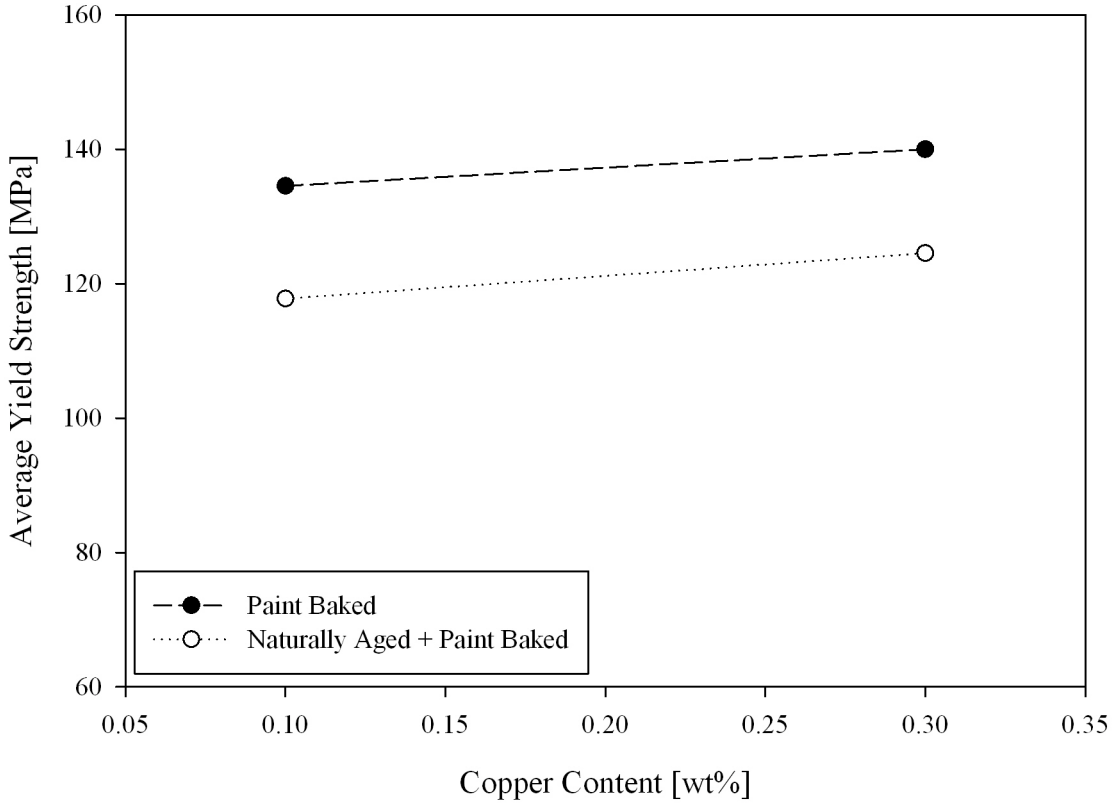

Figure 4.13. The effect of copper content on the paint bake strength with and without natural aging.

4.4 The Factors Affecting the Paint Bake Response

Figure 4.14 shows the paint bake response after natural aging with and without cold working. It can be seen that the increase in strength is nearly uniform for all the alloys, only being slightly greater for those with low magnesium levels (OEH, OEK, OEL, OEN). The average paint bake response with no applied strain is 17.1 MPa, which compares well with the values reported by other authors. Bottema *et al.* [33]

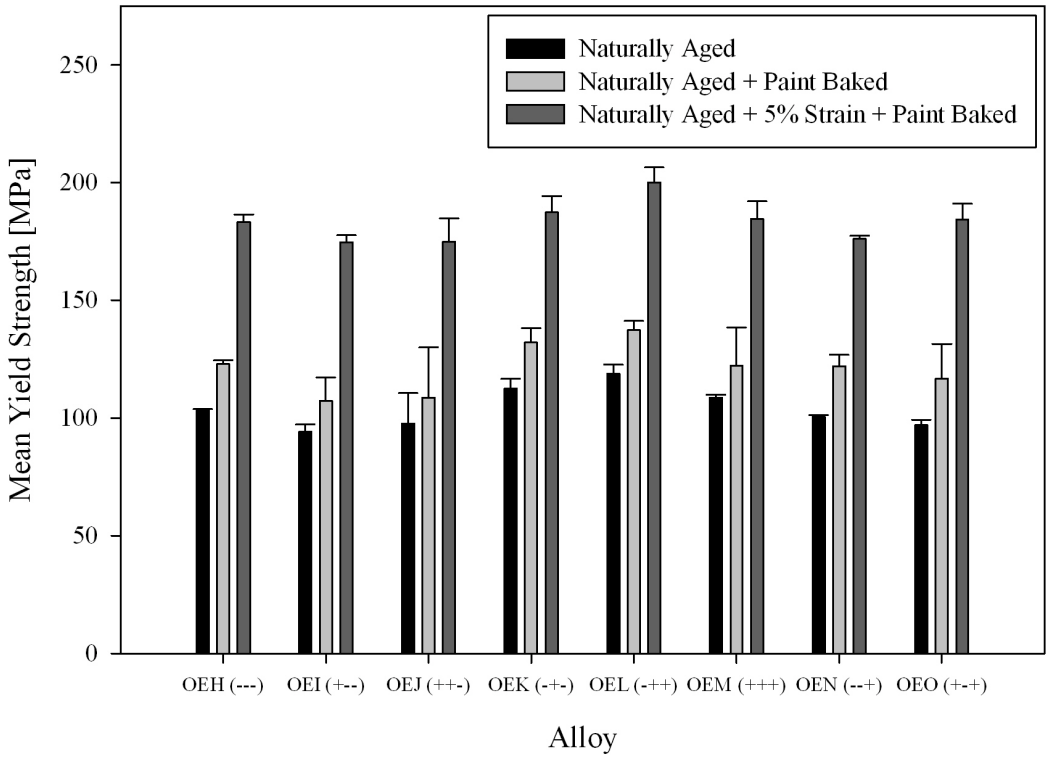

Figure 4.14. The paint bake response after natural aging with and without cold working.

found a paint bake response of approximately 23 MPa for a AA6016 alloy aged 30 minutes at 175 °C. Bryant [41] reported an average paint bake response of 20 MPa in the AA6111 alloy he studied. The application of strain prior to the paint bake process increases the yield strength of all the alloys, approximately 79 MPa on average. This appears to agree well with other reports of the paint bake response after strains of 2% were applied. Birol *et al.* [27] reported an increase of 35 MPa in AA6016 alloy. Hirth *et al.* [45] reported an increase of 70 MPa in both AA6016 and AA6111 alloys. In copper-free AA6022 alloy, Ji *et al.* [40] found an increase of approximately 31 MPa.

However, when 0.3 wt.% copper was added to the same alloy, the increase in strength jumped to almost 40 MPa. It should be noted the increase after 2% should be slightly less than that after 5%, as tested in this study.

The strength of the alloys in the naturally aged and paint baked condition is relatively low in the unstrained state. Automotive manufacturers would like the sheet products to have a minimum yield strength of 160 MPa after the paint bake process [38]. In order to achieve these levels, the paint bake response would have to be improved, likely through a pre-aging or pre-straining treatment.

4.5 The Formability of the Alloys Studied

The final strength of the products is one of the most important factors for automotive sheets. However, manufacturers must also take the formability of the sheet in the T4 condition prior to forming operations into consideration. If the sheet suffers from too much spring back or is not ductile enough, it either cannot be formed into the shapes necessary or it will suffer from cosmetic deficiencies such as surface roughening. As a result, manufacturers have suggested that aluminum sheets used for outer panels should feature a percent elongation of at least 24 percent [38, 45, 46]. Table 4.3 shows the percent elongation values (50 mm gauge length) for the alloys studied in the T4 condition. It can be seen that most of the alloys fall below this requirement. The formability of the alloys studied must be improved if they are to be used in industry as an option for automotive sheet applications.

Table 4.3. Percent elongation of naturally aged specimens (± denotes standard deviation).

	Alloy							
	OEH	OEI	OEJ	OEK	OEL	OEM	OEN	OEO
% Elongation	23.88 ± 2.31	15.42 ± 0.74	19.16 ± 2.35	19.55 ± 2.01	21.26 ± 2.58	18.11 ± 2.39	25.91 ± 0.75	17.58 ± 2.51

4.6 The Factors Affecting Ultimate Tensile Strength

Although the primary focus of this work is on the effect the composition and thermomechanical treatments had on the yield strength of the different alloys, a look at their effect on the ultimate tensile strength (UTS) is also warranted. Figure 4.15 shows the ultimate tensile stress for each alloy composition and thermomechanical treatment. It can be seen that the values are all relatively grouped together and the overall variation is not great.

Both hardness and strength measure a material's resistance to deformation, so it follows that there should be some relationship between the two. In the case of aluminum alloys, the relationship between hardness and ultimate tensile stress is:

$$UTS = 4.2 * HB \quad \text{..... (4.2)}$$

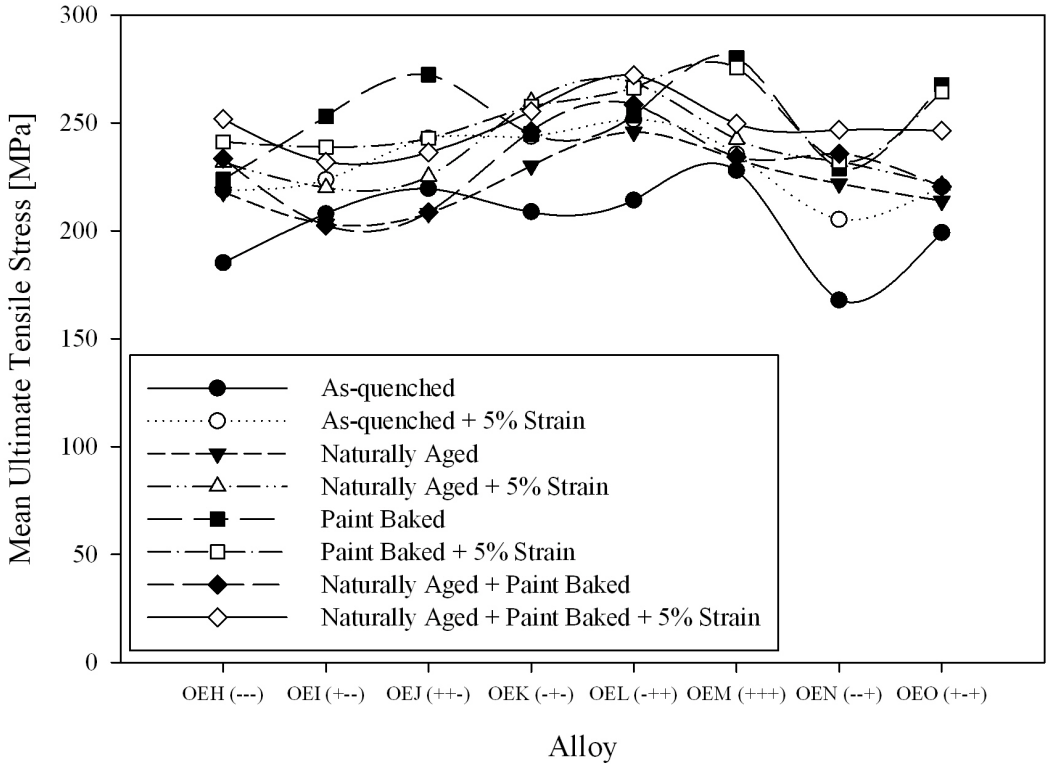

Figure 4.15. Variation of ultimate tensile stress.

where *HB* is the Brinell hardness of the material. Figure 4.16 compares the ultimate tensile strength of the naturally aged alloys studied based on equation (4.2) and the strength that was actually measured. As expected, the actual and predicted strengths are quite similar.

Table 4.4 lists the primary and interaction factors that most greatly affect the ultimate tensile strength as determined through the statistical analysis using the JMP 8 software. The prediction equation generated is given in equation (4.3).

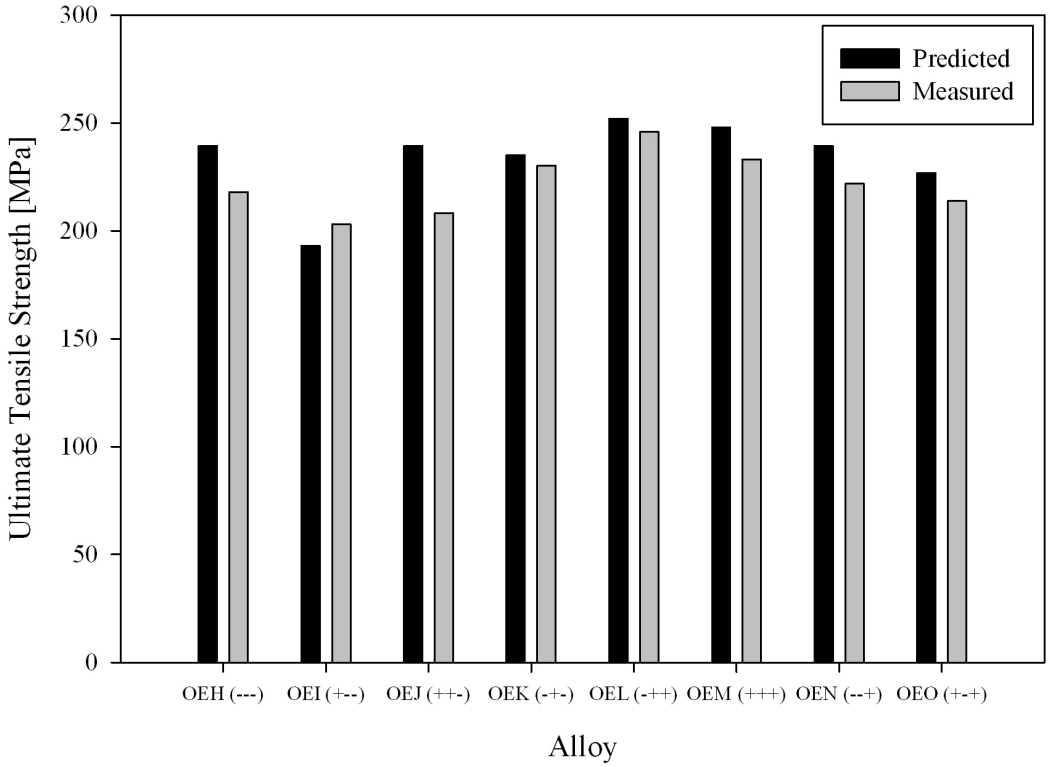

Figure 4.16. Comparison of predicted and ultimate tensile strengths for naturally aged samples.

Table 4.4. Primary factors affecting ultimate tensile strength.

Rank	Type	Factor(s)	Effect [MPa]
1	Primary	Paint Bake	± 11.34
2	Primary	Si	± 9.42
3	Interaction	Natural Aging * Mg	± 8.42
4	Primary	5% Strain	± 7.55
5	Interaction	Paint Bake * Natural Aging	± 6.49
6	Primary	Cu	± 3.83
7	Interaction	5% Strain * Paint Bake * Natural Aging	± 3.77
8	Interaction	Mg * Si	± 3.17
9	Interaction	5% Strain * Natural Aging * Mg	± 3.03
10	Interaction	5% Strain * Paint Bake	± 3.02
11	Interaction	Si * Cu	± 2.61
12	Interaction	5% Strain * Mg	± 2.38
13	Interaction	Mg * Cu	± 2.26
14	Interaction	Paint Bake * Cu	± 2.15

$$
\begin{aligned}
UTS = {} & 234.694 \\
& + 9.424 * \left[\frac{(Si) - 0.75}{0.15} \right] \\
& + \left[\frac{(Mg) - 0.65}{0.15} \right] * \left[\frac{(Si) - 0.75}{0.15} \right] * -3.165 \\
& + 3.833 * \left[\frac{(Cu) - 0.20}{0.10} \right] \\
& + \left[\frac{(Mg) - 0.65}{0.15} \right] * \left[\frac{(Cu) - 0.20}{0.10} \right] * 2.263 \\
& + \left[\frac{(Si) - 0.75}{0.15} \right] * \left[\frac{(Cu) - 0.20}{0.10} \right] * 2.611 \\
& + Match(\text{Natural Aging}) \begin{bmatrix} "No" \Rightarrow \left[\frac{(Mg) - 0.65}{0.15} \right] * 8.426 \\ "Yes" \Rightarrow \left[\frac{(Mg) - 0.65}{0.15} \right] * -8.426 \end{bmatrix} \\
& + Match(5\% \text{ Strain}) \begin{bmatrix} "No" \Rightarrow Match(\text{Natural Aging}) \begin{bmatrix} "No" \Rightarrow \left[\frac{(Mg) - 0.65}{0.15} \right] * 3.032 \\ "Yes" \Rightarrow \left[\frac{(Mg) - 0.65}{0.15} \right] * -3.032 \end{bmatrix} \\ "Yes" \Rightarrow Match(\text{Natural Aging}) \begin{bmatrix} "No" \Rightarrow \left[\frac{(Mg) - 0.65}{0.15} \right] * -3.032 \\ "Yes" \Rightarrow \left[\frac{(Mg) - 0.65}{0.15} \right] * 3.032 \end{bmatrix} \end{bmatrix} \quad \ldots\ldots. (4.3) \\
& + Match(\text{Paint Bake}) \begin{bmatrix} "No" \Rightarrow -11.339 \\ "Yes" \Rightarrow +11.339 \end{bmatrix} \\
& + Match(\text{Paint Bake}) \begin{bmatrix} "No" \Rightarrow \left[\frac{(Cu) - 0.20}{0.10} \right] * -2.142 \\ "Yes" \Rightarrow \left[\frac{(Cu) - 0.20}{0.10} \right] * 2.142 \end{bmatrix} \\
& + Match(5\% \text{ Strain}) \begin{bmatrix} "No" \Rightarrow Match(\text{Paint Bake}) \begin{bmatrix} "No" \Rightarrow -3.020 \\ "Yes" \Rightarrow 3.020 \end{bmatrix} \\ "Yes" \Rightarrow Match(\text{Paint Bake}) \begin{bmatrix} "No" \Rightarrow 3.020 \\ "Yes" \Rightarrow -3.020 \end{bmatrix} \end{bmatrix}
\end{aligned}
$$

*continued on the next page.

$$
\begin{aligned}
&+Match(\text{Paint Bake})\begin{bmatrix} \text{"}No\text{"} \Rightarrow Match(\text{Natural Aging})\begin{bmatrix} \text{"}No\text{"} \Rightarrow -6.486 \\ \text{"}Yes\text{"} \Rightarrow 6.486 \end{bmatrix} \\ \text{"}Yes\text{"} \Rightarrow Match(\text{Natural Aging})\begin{bmatrix} \text{"}No\text{"} \Rightarrow 6.486 \\ \text{"}Yes\text{"} \Rightarrow -6.486 \end{bmatrix} \end{bmatrix} \\
&+Match(5\%\ \text{Strain})\begin{bmatrix} \text{"}No\text{"} \Rightarrow Match(\text{Paint Bake})\begin{bmatrix} \text{"}No\text{"} \Rightarrow Match(\text{Natural Aging})\begin{bmatrix} \text{"}No\text{"} \Rightarrow -3.765 \\ \text{"}Yes\text{"} \Rightarrow 3.765 \end{bmatrix} \\ \text{"}Yes\text{"} \Rightarrow Match(\text{Natural Aging})\begin{bmatrix} \text{"}No\text{"} \Rightarrow 3.765 \\ \text{"}Yes\text{"} \Rightarrow -3.765 \end{bmatrix} \end{bmatrix} \\ \text{"}Yes\text{"} \Rightarrow Match(\text{Paint Bake})\begin{bmatrix} \text{"}No\text{"} \Rightarrow Match(\text{Natural Aging})\begin{bmatrix} \text{"}No\text{"} \Rightarrow 3.765 \\ \text{"}Yes\text{"} \Rightarrow -3.765 \end{bmatrix} \\ \text{"}Yes\text{"} \Rightarrow Match(\text{Natural Aging})\begin{bmatrix} \text{"}No\text{"} \Rightarrow -3.765 \\ \text{"}Yes\text{"} \Rightarrow 3.765 \end{bmatrix} \end{bmatrix} \end{bmatrix}
\end{aligned}
$$

where *UTS* is the predicted ultimate tensile strength, and *(Mg)*, *(Si)*, and *(Cu)* represent the composition level of magnesium, silicon, and copper respectively.

The majority of the factors that most greatly influenced the mean yield strength also appreciably affect the ultimate tensile stress. However, the degree to which they may affect the ultimate tensile stress is different. By examining each factor and the effect it has on the predicted ultimate tensile strength, the optimum combination of composition and treatments can be determined. It can be assumed that some natural aging will occur as it is nearly unavoidable in industry, and there will also be a paint bake treatment applied. Given these conditions, the highest ultimate tensile strength is obtained when magnesium is at a low level (i.e., 0.5 wt.%) and silicon and copper are both at their high levels (i.e., 0.9 wt.% and 0.3 wt.%, respectively). This agrees with the findings for the yield strength.

4.7 An Examination of the Grain Morphology

An attempt was made during this study to characterize the grain morphology of every configuration tested. That is, each combination of composition and thermomechanical treatment. Unfortunately, not every specimen could be etched, and a complete summary was not obtained. Some very good results were produced for those samples that received artificial aging through the simulated paint bake. For reasons unknown, samples that did not undergo the paint bake were etched with a very low success rate. Complete data was obtained for those specimens that received only artificial aging, and also those that received both natural and artificial aging. The cold worked samples examined were strained at 10 percent. This high level of strain was used because it would ensure a significant difference between strained and unstrained. Table 4.5 summarizes ASTM grain sizes for these samples. The range of grain sizes, say 4.0 to 6.0, corresponds to an mean intercept length of 80 μm to 40 μm, respectively. It can be seen that the application of strain prior to the paint bake treatment leads to a smaller average grain size.

Table 4.5 Average ASTM grain sizes of select samples.

Composition	Treatment			
	Paint Baked	10% Strain + Paint Baked	Naturally Aged + Paint Baked	10% Strain + Naturally Aged + Paint Baked
OEH	5.00	5.75	4.90	5.16
OEI	4.14	3.45	4.20	4.24
OEJ	4.70	4.49	4.39	5.22
OEK	4.91	5.85	5.15	5.96
OEK	4.24	4.68	4.89	5.50
OEM	4.57	6.27	4.47	5.19
OEN	4.45	5.54	5.15	5.36
OEO	5.24	5.35	4.24	4.71
Average	4.66	5.17	4.67	5.17

Figures 4.17 and 4.18 show a micrograph from a specimen of each treatment highlighted in Table 4.5. Each appears to consist of randomly oriented, equiaxed grains.

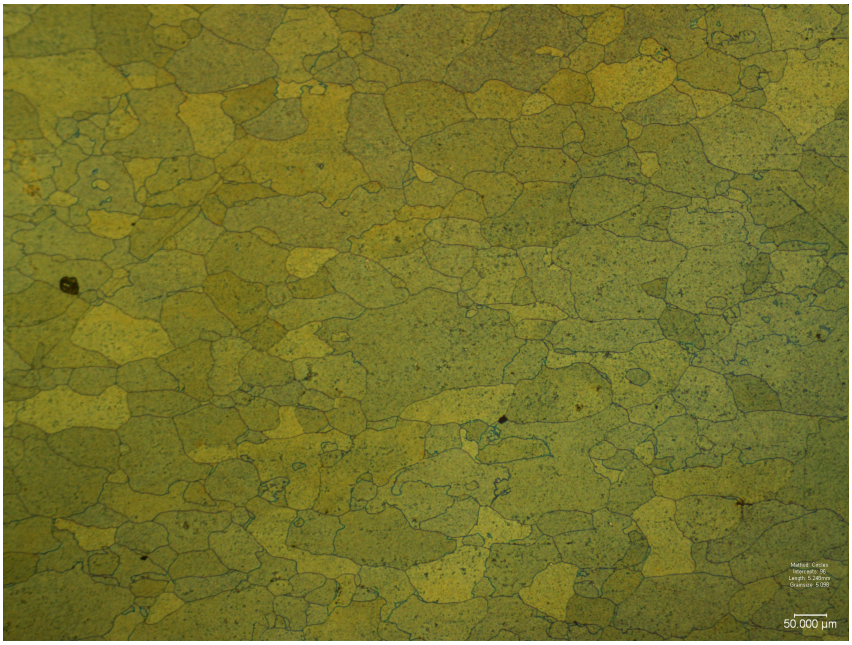

(a)

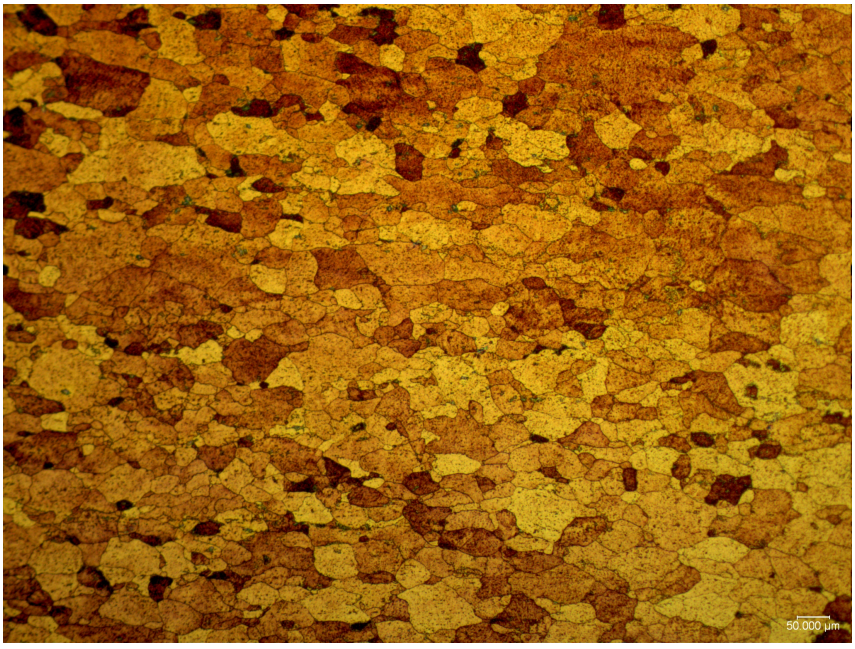

(b)

Figure 4.17. Micrographs of selected samples. (a) OEO paint baked; and (b) OEM 10% strain + paint baked.

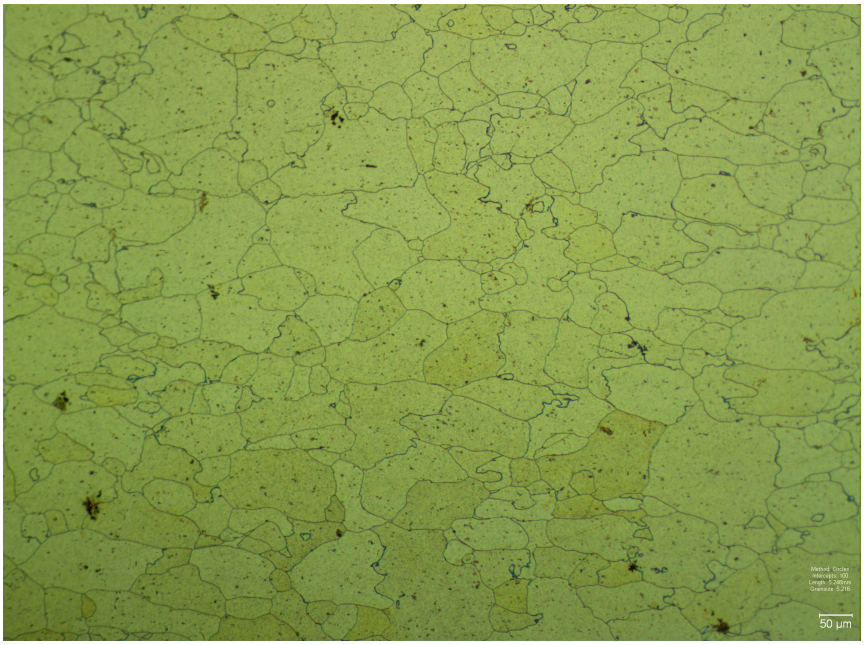

(a)

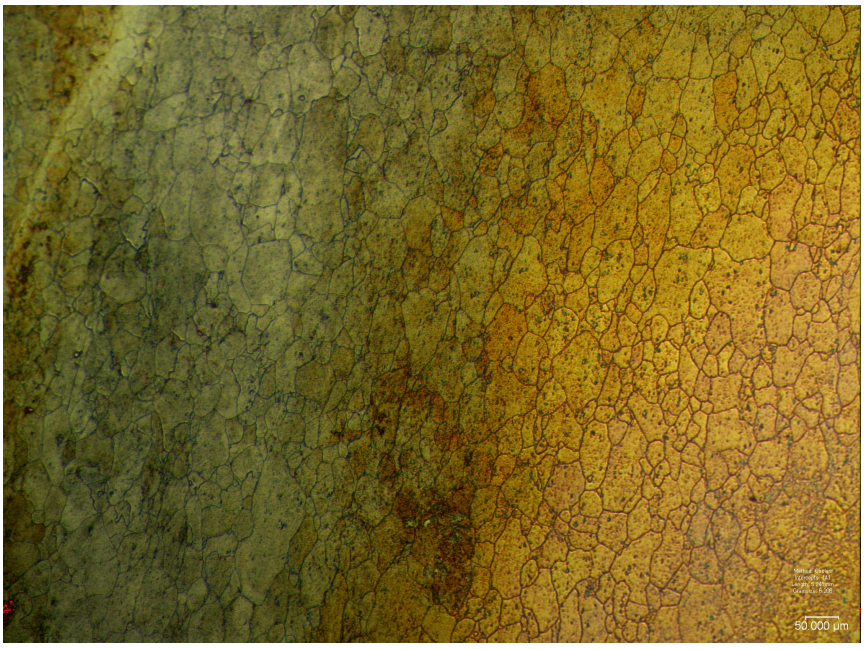

(b)

Figure 4.18. Micrographs of selected samples. (a) OEH naturally aged + paint baked; and (b) OEK 10% strain + naturally aged + paint baked.

5 CONCLUSIONS AND RECOMMENDATIONS

In this study the effects of solute concentration and thermomechanical treatments on the strength of a group of copper-containing Al-Mg-Si alloys were studied using different experimental techniques. The techniques used included microhardness measurements, tensile testing, and optical metallography. Based on the results presented in Chapter 4, the following conclusions can be made.

5.1 Conclusions

1. Natural aging occured rapidly in the alloys examined, with the majority of the hardening occurring within the first 24 hours.

2. Cold work prior to the final paint bake appreciably increased the yield strength in the alloys tested.

3. Artificial aging during the automotive paint bake cycle increased the yield strength of each alloy. The degree of strengthening varied with composition.

4. Natural aging degraded the paint bake response of all the alloys with high magnesium contents (i.e., 0.8 wt.%).

5. On the average, the alloys examined with high silicon content have higher yield strengths than those with low silicon content.

6. Increase in copper content reduced the degradation of the paint bake response caused by natural aging.

7. The highest strength levels in the naturally aged and paint baked condition were achieved when magnesium levels are low (i.e., 0.5 wt.%) and both silicon and copper levels are high (i.e., 0.9 and 0.3 wt.%, respectively).

8. Weck's reagent was only effective in revealing grain boundaries in those specimens that were subjected to the paint bake treatment. Very little success was had with specimens that were not artificially aged.

5.2 Recommendations for Future Work

1. The effect of a pre-aging or pre-straining treatment performed prior to the paint bake procedure should be investigated. Specifically, the effect it might have on final strength (paint bake response).

2. The overall effect of the various factors was determined, but the exact cause of the results was undetermined. A study of the microstructures and the

precipitation products would help determine these causes. This could include using DSC, XRD, and electron microscopy techniques to determine the precipitate morphology and the precipitation sequence.

3. Corrosion resistance is very important in the automotive industry. A corrosion study of the various alloys examined is needed to determine the effect the solute concentration and thermomechanical treatments have on the overall corrosion resistance.

REFERENCES

1. National Research Council Committee on the Effectiveness and Impact of Corporate Average Fuel Economy (CAFE) Standards, *Effectiveness and Impact of Corporate Average Fuel Economy (CAFE) Standards*. Washington D.C.: National Academy Press, 2002.
2. National Highway Traffic Safety Administration, "CAFE Overview - Frequently Asked Questions." vol. 2008: *National Highway Traffic Safety Administration*, 2007. [Online]. Available: http://www.nhtsa.dot.gov. [Accessed: July 2008].
3. A. Steffan, "My Other Car is a Bright Green City," in *World Changing*, January 2008. [Online]. Available: http://www.worldchanging.com. [Accessed: July 2008].
4. D. L. Greene and N. I. Tishchishyna, "Cost of Oil Dependence: A 2000 Update," Oak Ridge National Laboratory, Tennessee, United States, Technical Report ORNL/TM-2000/152, 2000.
5. A. Bandivadekar, *et al.*, "On the Road in 2035: Reducing Transportation's Petroleum Consumption and GHG Emissions," Massachusetts Institute of Technology, Cambridge, MA, United States, Report No. LFEE 2008-05 RP, 2008.
6. L. Cheah, C. Evans, A. Bandivadekar, and J. Heywood, "Factor of Two: Halving the Fuel Consumption of New U.S. Automobiles by 2035," Massachusetts Institute of Technology, Cambridge, MA, United States, Report No. LFEE 2007-04 RP, 2007.
7. F. Stodolsky, A. Vyas, R. Cuenca, and L. Gaines, "Life-Cycle Energy Savings Potential from Aluminum-Intensive Vehicles," presented at 1995 Total Life Cycle Conference & Exposition, Vienna, Austria, 1995.
8. W. S. Miller, L. Zhuang, J. Bottema, and A. J. Wittebrood, "Recent development in aluminium alloys for the automotive industry," *Materials Science & Engineering A,* vol. 280, pp. 37-49, January 2000.
9. I. N. Fridlyander, V. G. Sister, and O. E. Grushko, "Aluminum Alloys: Promising Materials in the Automotive Industry," *Metal Science and Heat Treatment,* vol. 44, pp. 365-370, January 2002.
10. E. Brünger, O. Engler, and J. Hirsch, "Al-Mg-Si sheet alloys for autobody applications," in *Virtual Fabrication of Aluminum Products: Microstructural Modeling in Industrial Aluminium Fabrication Processess*, J. Hirsch, Ed. Weinheim, Germany: Wiley-VCH, 2006, pp. 51-61.
11. D. A. Buckingham, "Aluminum Stocks in Use in Automobiles in the United States," *United States Geological Survey,* 2006. [Online]. Available: http://pubs.usgs.gov/fs/2005/3145. [Accessed: July 2008].

12. J. Hirsch, "Automotive Trends in Aluminum - The European Perspective," *Materials Forum,* vol. 28, pp. 15-23, 2004.
13. S. Murtha, "New 6xxx Aluminum Alloy for Automotive Body Sheet Applications," *SAE Transactions,* pp. 657-666, 1995.
14. S. O. Kasap, *Principles of Electronic Materials and Devices*, 3rd ed. New York, NY: McGraw-Hill, 2006.
15. W. D. Callister Jr., *Materials Science and Engineering: An Introduction*, 6th ed. New York, NY: John Wiley & Sons, Inc., 2003.
16. G. K. Quainoo, "The effect of cold work on precipitation in AA6111 aluminum," Ph.D. thesis, University of Saskatchewan, Saskatoon, SK, Canada, 2004.
17. G. Burger, A. Gupta, P. Jeffrey, and D. Lloyd, "Microstructural Control of Aluminum Sheet Used in Automotive Applications," *Materials Characterization,* vol. 35, pp. 23-39, July 1995.
18. M. Warmuzek, "Metallographic Techniques for Aluminum and Its Alloys," in *ASM Handbook Volume 9: Metallography and Microstructures*. vol. 9, G. VanderVoort, Ed. Materials Park, OH: ASM International, 2004, pp. 711-720.
19. K. G. Budinski and M. K. Budinski, *Engineering Materials: Properties and Selection*, 8th ed. Upper Saddle River, NJ: Pearson Prentice Hall, 2005.
20. W. F. Miao and D. E. Laughlin, "Effects of Cu content and preaging on precipitation characteristics in aluminum alloy 6022," *Metallurgical and Materials Transactions A,* vol. 31, pp. 361-371, February 2000.
21. S. Esmaeili, X. Wang, D. Lloyd, and W. Poole, "On the precipitation-hardening behavior of the Al-Mg-Si-Cu alloy AA6111," *Metallurgical and Materials Transactions A,* vol. 34, pp. 751-763, March 2003.
22. X. Wang, J. D. Embury, W. J. Poole, S. Esmaeili, and D. J. Lloyd, "Precipitation strengthening of the aluminum alloy AA6111," *Metallurgical and Materials Transactions A,* vol. 34, pp. 2913-2924, December 2003.
23. G. Edwards, K. Stiller, G. L. Dunlop, and M. J. Couper, "The precipitation sequence in Al–Mg–Si alloys," *Acta Materialia,* vol. 46, pp. 3893-3904, July 1998.
24. A. Perovic, D. D. Perovic, G. C. Weatherly, and D. J. Lloyd, "Precipitation in aluminum alloys AA6111 and AA6016," *Scripta Materialia,* vol. 41, pp. 703-708, August 1999.
25. D. Chakrabarti and D. E. Laughlin, "Phase relations and precipitation in Al–Mg–Si alloys with Cu additions," *Progress in Materials Science,* vol. 49, no. 3-4, pp. 389-410, 2004.
26. R. S. Yassar, D. P. Field, and H. Weiland, "The effect of predeformation on the β″and β′ precipitates and the role of Q′ phase in an Al–Mg–Si alloy; AA6022," *Scripta Materialia,* vol. 53, pp. 299-303, August 2005.
27. J. Bryant, "The Effects of Preaging Treatments on Aging Kinetics and Mechanical Properties in AA6111 Aluminum Autobody Sheet," *Metallurgical and Materials Transactions A,* vol. 30, pp. 1999-2006, August 1999.
28. W. F. Miao and D. E. Laughlin, "Precipitation Hardening in Aluminum Alloy 6022," *Scripta Materialia,* vol. 40, pp. 873-878, March 1999.

29. T. Moons, P. Ratchev, P. De Smet, B. Verlinden, and P. Van Houtte, "A comparative study of two Al-Mg-Si alloys for automotive applications," *Scripta Materialia,* vol. 35, pp. 939-945, October 1996.
30. Y. Birol and M. Karlík, "Bake hardening of twin roll cast Al-Mg-Si sheet," *Materials Science and Technology,* vol. 21, pp. 153-158, August 2005.
31. Y. An, L. Zhuang, H. Vegter, and A. Hurkmans, "Fast Aging Kinetics of the AA6016 Al-Mg-Si Alloy and the Application in Forming Process," *Metallurgical and Materials Transactions A,* vol. 33, pp. 3121-3126, October 2002.
32. Y. Birol and M. Karlik, "The interaction of natural ageing with straining in a twin-roll cast AlMgSi automotive sheet," *Scripta Materialia,* vol. 55, pp. 625-628, October 2006.
33. M. Murayama, K. Hono, W. Miao, and D. Laughlin, "The effect of Cu additions on the precipitation kinetics in an Al-Mg-Si alloy with excess Si," *Metallurgical and Materials Transactions A,* vol. 32, pp. 239-246, February 2001.
34. J. Dutkiewicz and L. Litynska, "The effect of plastic deformation on structure and properties of chosen 6000 series aluminium alloys," *Materials Science & Engineering A,* vol. 324, pp. 239-243, February 2002.
35. M. Murayama and K. Hono, "Pre-precipitate clusters and precipitation processes in Al–Mg–Si alloys," *Acta Materialia,* vol. 47, pp. 1537-1548, March 1999.
36. M. Murayama, K. Hono, M. Saga, and M. Kikuchi, "Atom probe studies on the early stages of precipitation in Al-Mg-Si alloys," *Materials Science and Engineering-A-Structural Materials,* vol. 250, pp. 127-132, July 1998.
37. S. P. Ringer and K. Hono, "Microstructural Evolution and Age Hardening in Aluminum Alloys: Atom Probe Field-Ion Microscopy and Transmission Electron Micrscopy Studies," *Materials Characterization,* vol. 44, pp. 101-131, January-February 2000.
38. Y. Ji, F. Guo, and Y. Pan, "Microstructural characteristics and paint-bake response of Al-Mg-Si-Cu alloy," *Transactions of Nonferrous Metals Society of China,* vol. 18, pp. 126-131, February 2008.
39. A. K. Gupta, D. J. Lloyd, and S. A. Court, "Precipitation hardening in Al–Mg–Si alloys with and without excess Si," *Materials Science & Engineering A,* vol. 316, pp. 11-17, November 2001.
40. S. M. Hirth, G. J. Marshall, S. A. Court, and D. J. Lloyd, "Effects of Si on the aging behaviour and formability of aluminium alloys based on AA6016," *Materials Science & Engineering A,* vol. 319-321, pp. 452-456, December 2001.
41. J. Bottema, C. Lahaye, R. Baartman, L. Zhuang, P. DeSmet, and F. Schoepen, "Recent Developments in AA6016 Aluminum Type Body Sheet Products," *SAE Transactions,* pp. 900-906, 1998.
42. E. Tan and B. Ögel, "Influence of Heat Treatment on the Mechanical Properties of AA6066 Alloy," *Turkish Journal of Engineering and Environmental Science,* vol. 31, pp. 53-60, January 2007.

43. L. Zhen, W. D. Fei, S. B. Kang, and H. W. Kim, "Precipitation behaviour of Al–Mg–Si alloys with high silicon content," *Journal of Materials Science,* vol. 32, pp. 1895-1902, April 1997.
44. Y. Birol, "Pre-straining to improve the bake hardening response of a twin-roll cast Al–Mg–Si alloy," *Scripta Materialia,* vol. 52, pp. 169-173, February 2005.
45. Y. Birol, "Pre-aging to improve bake hardening in a twin-roll cast Al-Mg-Si alloy," *Materials Science and Engineering A,* vol. 391, pp. 175-180, January 2005.
46. M. Dündar and Y. Birol, "Formability of a Twin-Roll Cast AA 6016 Sheet for Automotive Applications," *Materials Forum,* vol. 28, pp. 646-651, 2004.

APPENDIX A

Procedure for Weck's Reagent

This appendix details the procedure used to etch the specimens with Weck's Reagent.

1) Ensure specimens have been well polished to a sub-micron finish.

2) Prepare Weck's Reagent by thoroughly dissolving 4 g potassium permanganate ($KMnO_4$) and 1 g sodium hydroxide (NaOH) in 100 mL of distilled water (H_2O).

3) Rinse the specimen under warm water to ensure a clean surface.

4) Rinse with methanol and dry.

5) Spray specimen with distilled water. Shake excess off.

6) Using tongs to hold the sample, immerse the polished surface in the reagent.

7) Agitate mildly (move the specimen around).

8) Remove specimen after approximately 20-30 seconds.

9) Triple rinse in water.

10) Rinse with methanol and dry.

11) Check under microscope for grain structure.

12) Repeat steps 5-11 if necessary, but only for a short time (i.e., ~5 seconds).

APPENDIX B

Stress-strain Curves

This appendix contains selected stress-strain curves obtained during tensile testing.

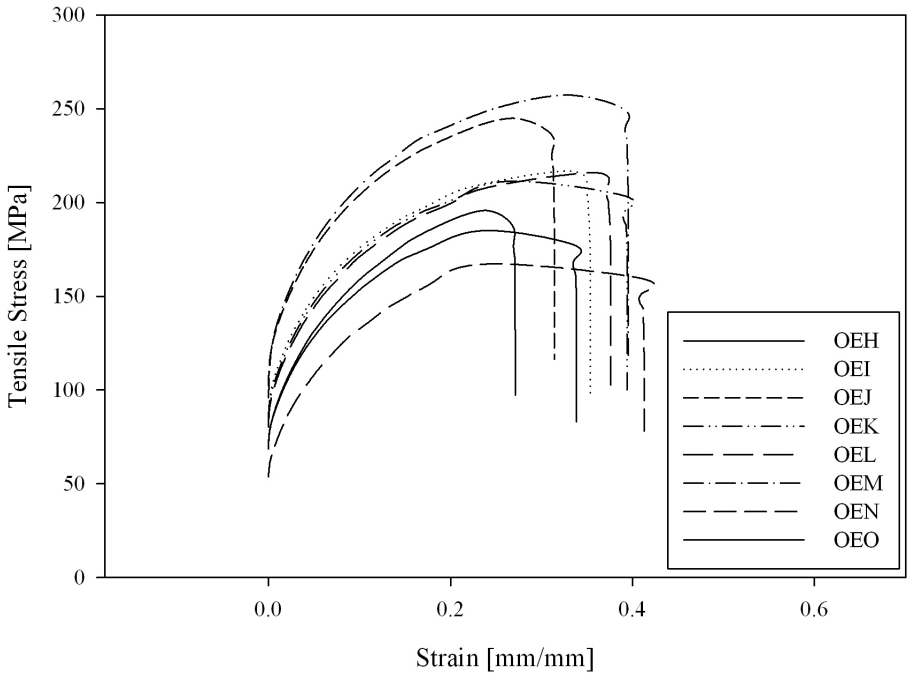

Figure B.1. Stress-strain curve for selected as-quenched samples.

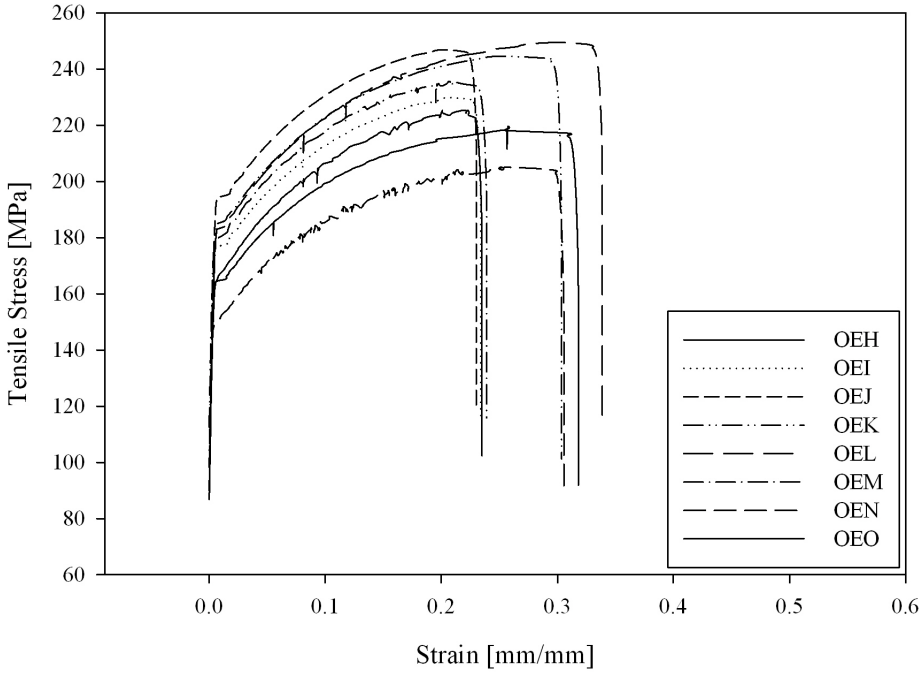

Figure B.2. Stress-strain curve for selected as-quenched samples with 5% strain.

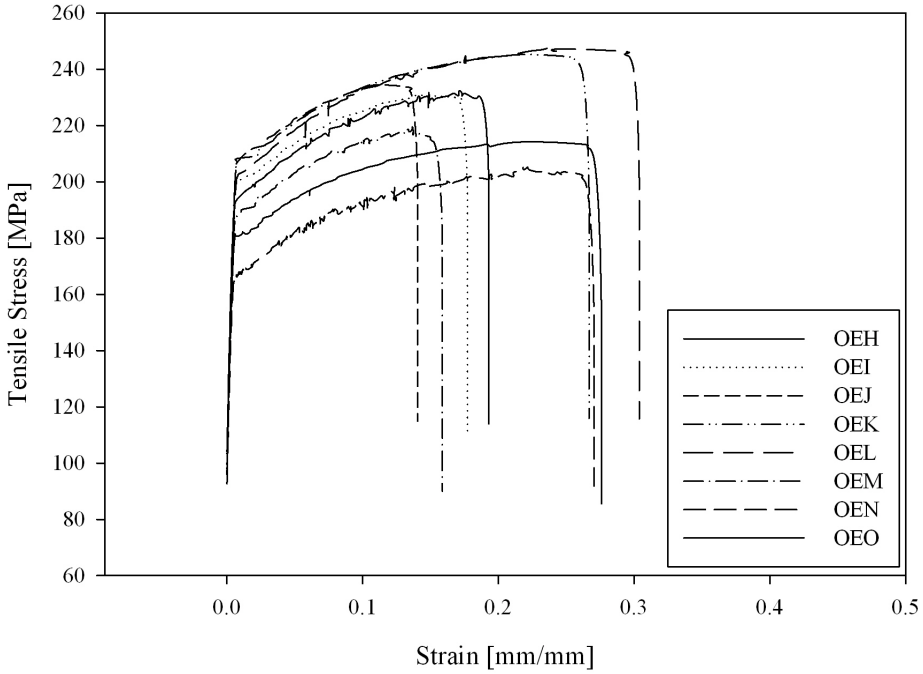

Figure B.3. Stress-strain curve for selected as-quenched samples with 10% strain.

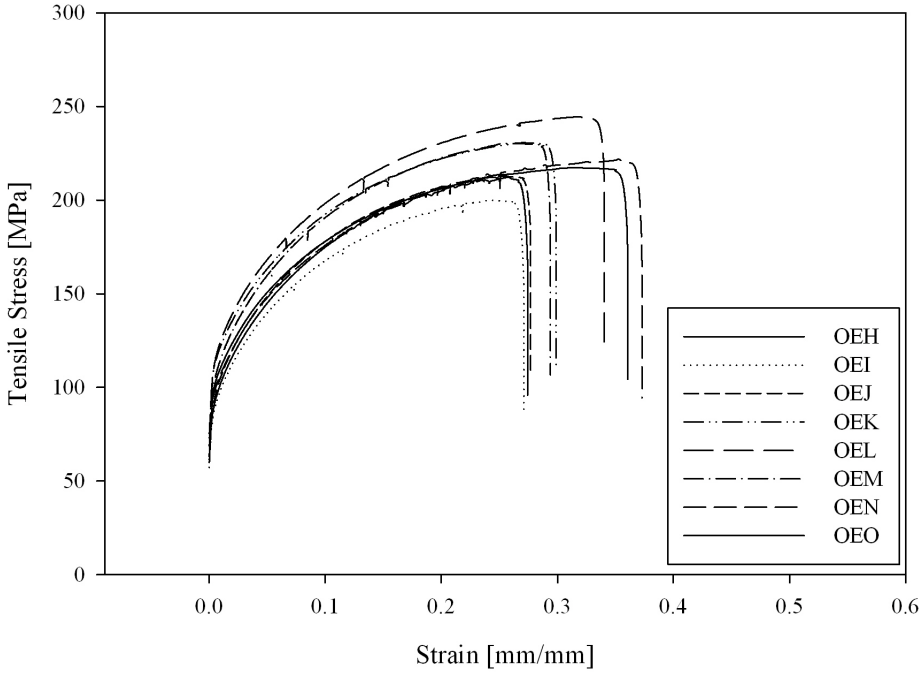

Figure B.4. Stress-strain curve for selected naturally aged samples.

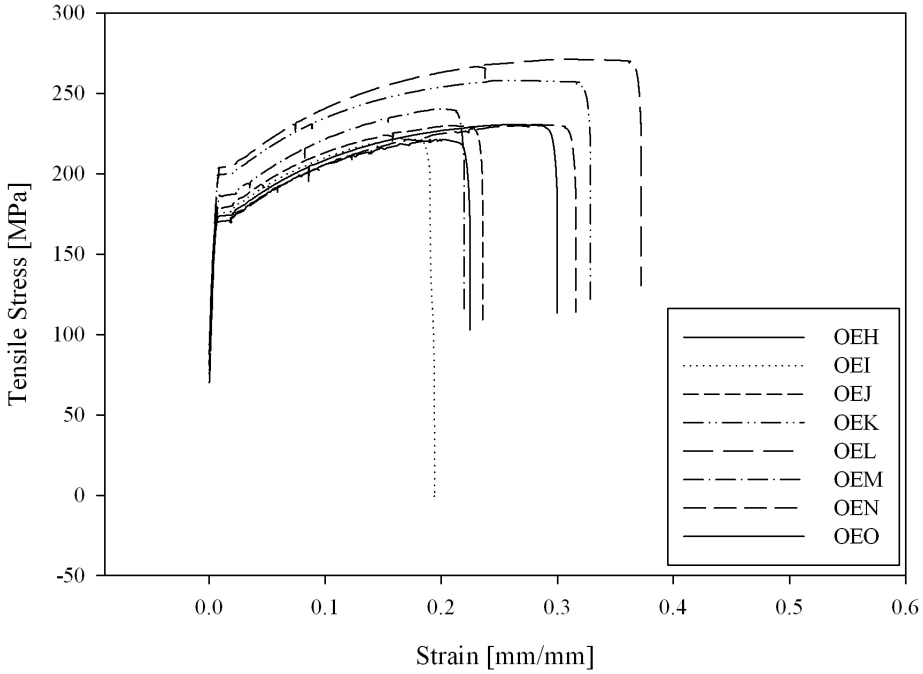

Figure B.5. Stress-strain curve for selected naturally aged samples with 5% strain.

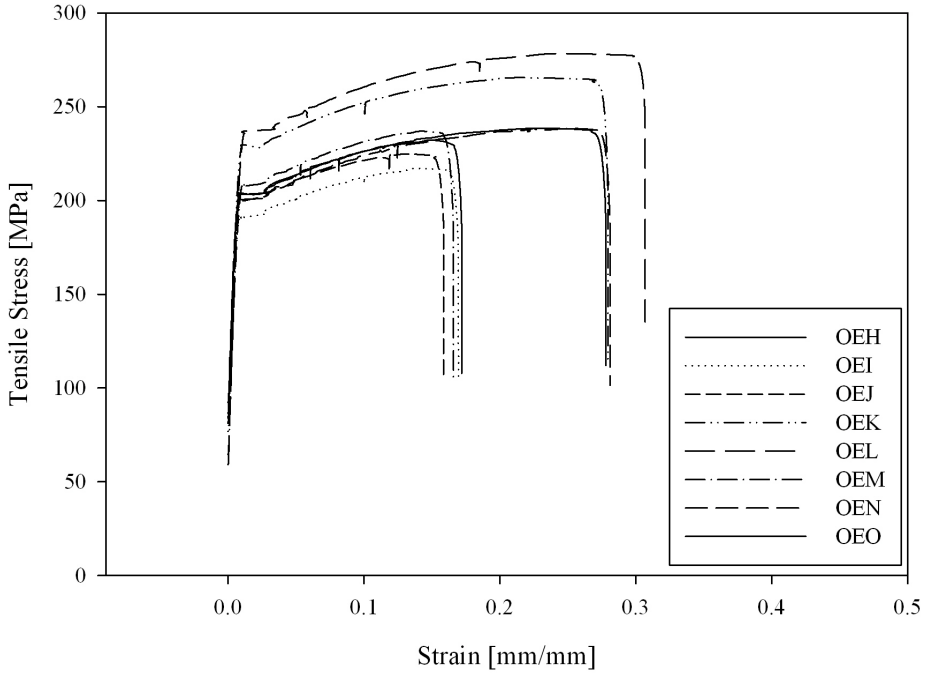

Figure B.6. Stress-strain curve for selected naturally aged samples with 10% strain.

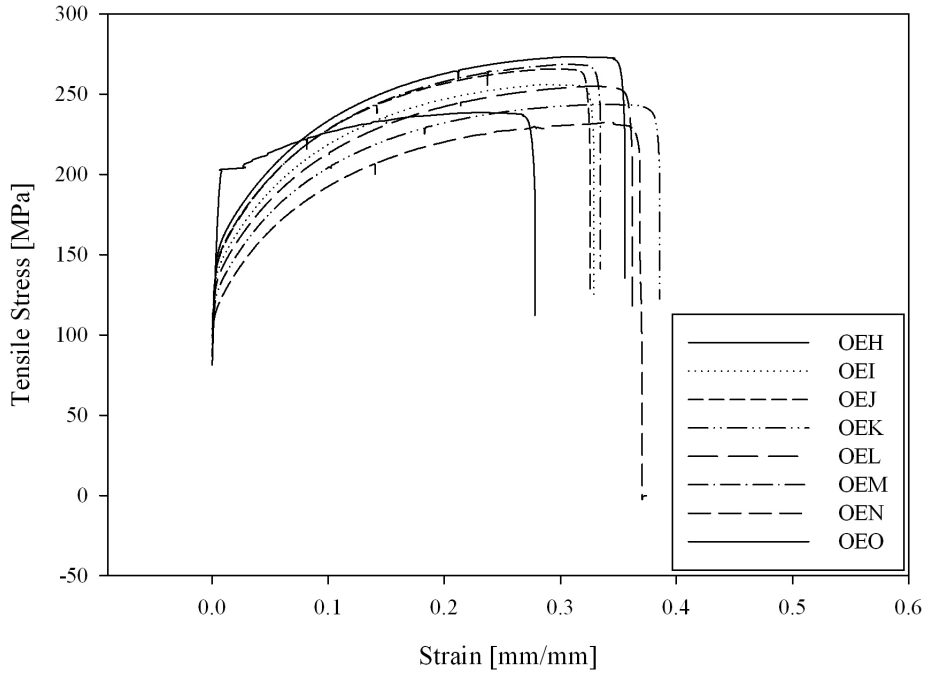

Figure B.7. Stress-strain curve for selected artificially aged samples.

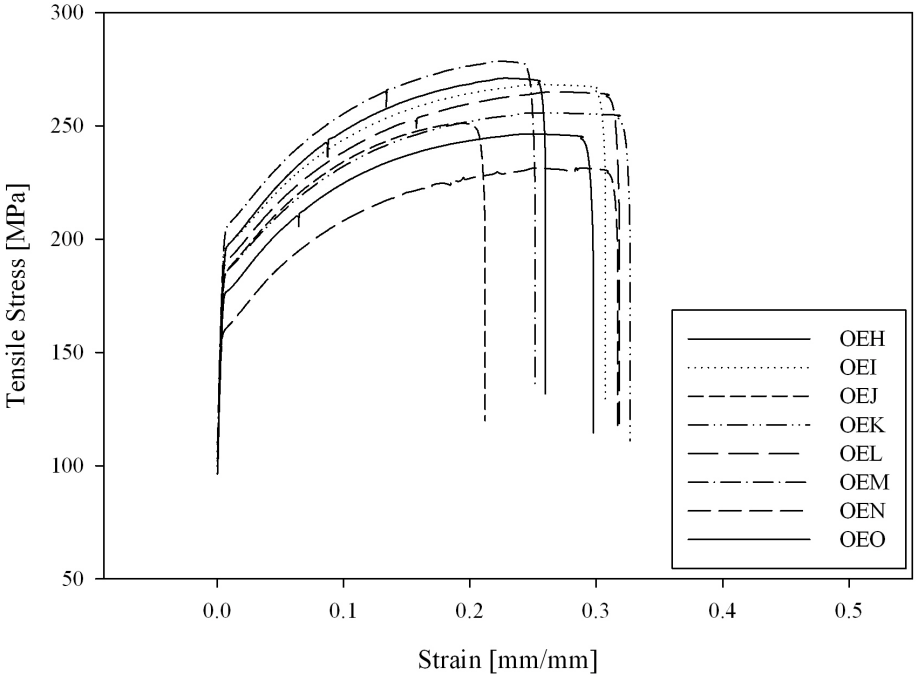

Figure B.8. Stress-strain curve for selected artificially aged samples with 5% strain.

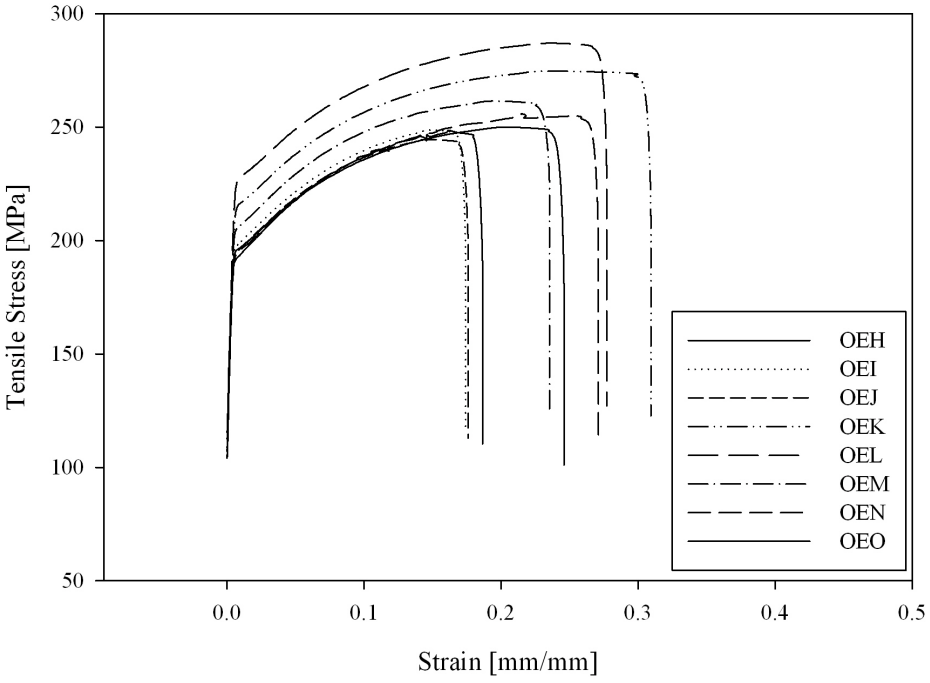

Figure B.9. Stress-strain curve for selected artificially aged samples with 10% strain.

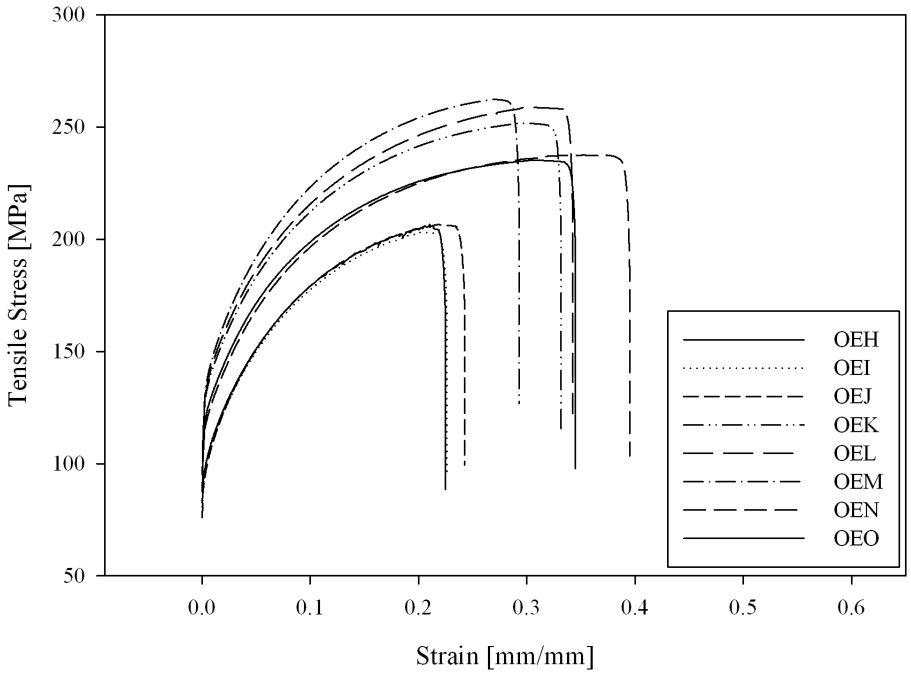

Figure B.10. Stress-strain curve for selected naturally and artificially aged samples.

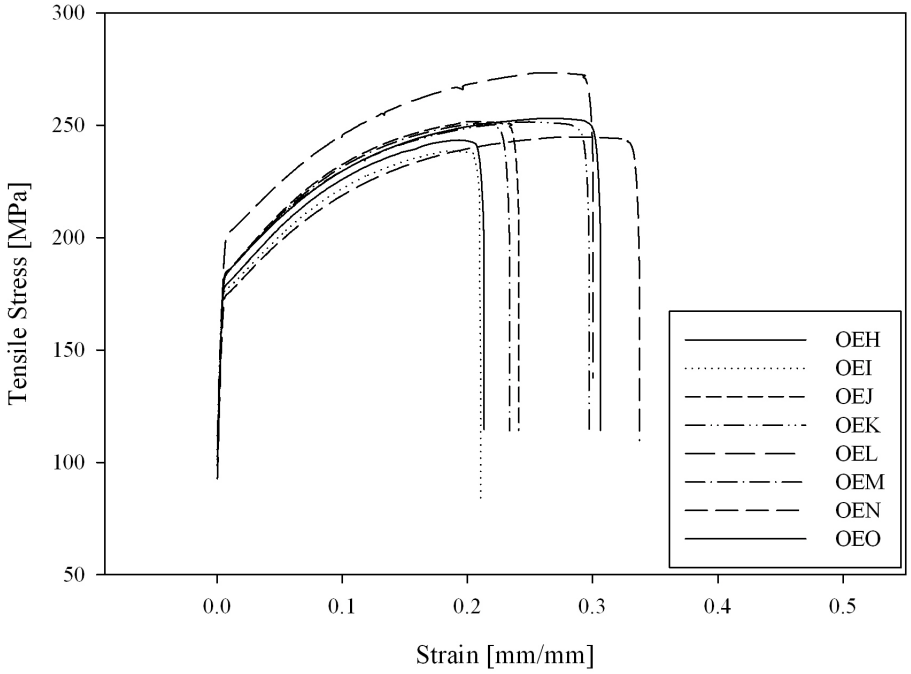

Figure B.11. Stress-strain curve for selected naturally and artificially aged samples with 5% strain.

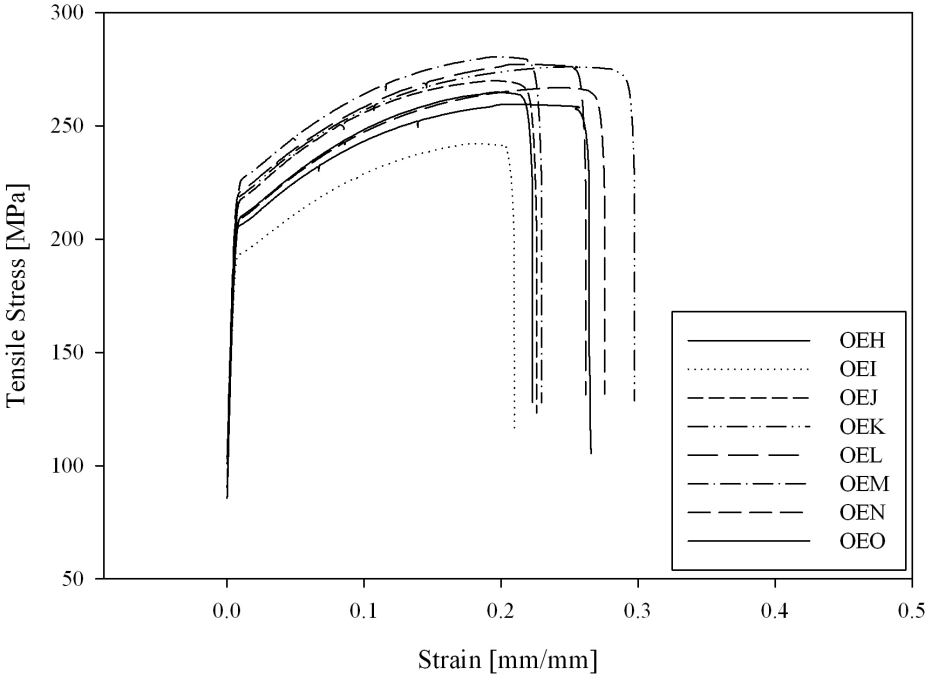

Figure B.12. Stress-strain curve for selected naturally and artificially aged samples with 10% strain.

APPENDIX C

Statistics for Primary Factors

This appendix contains the f-statistics related to the primary factors for the prediction model of the mean yield strength.

Table C.1. ANOVA table for mean yield strength prediction.

Source	Degrees of Freedom	Sum of Squares	Mean Square	F Ratio	Prob > F
Model	63	240658.89	3819.98		
Error	128	13971.49	109.15	34.9968	< 0.0001
Corrected Total	191	254630.38			

Table C.2. Effects tests used to determine the main factors.

Term	Sum of Squares	F Ratio	Prob > F
Mg (0.5, 0.8)	126.21	1.1563	0.2843
Si (0.6, 0.9)	9255.88	84.7979	< 0.0001
Mg * Si	1687.74	15.4622	0.0001
Cu (0.1, 0.3)	158.25	1.4498	0.2308
Mg * Cu	549.08	5.0304	0.0266
Si * Cu	844.83	7.7399	0.0062
Mg * Si * Cu	171.06	1.5672	0.2129
5% Strain (None)	195985.77	1795.526	< 0.0001
5% Strain * Mg	119.69	1.0965	0.2970
5% Strain * Si	197.70	1.8112	0.1807
5% Strain * Mg * Si	131.66	1.2062	0.2742
5% Strain * Cu	0.37	0.0034	0.9539
5% Strain * Mg * Cu	13.16	0.1206	0.7290
5% Strain * Si * Cu	74.46	0.6822	0.4104
5% Strain * Mg * Si * Cu	30.50	0.2795	0.5980
Natural Aging (None)	111.10	1.0178	0.3149
Natural Aging * Mg	6352.03	58.1942	< 0.0001
Natural Aging * Si	404.99	3.7103	0.0563
Natural Aging * Mg * Si	1.84	0.0168	0.8969

Term	Sum of Squares	F Ratio	Prob > F
Natural Aging * Cu	386.72	3.5430	0.0621
Natural Aging * Mg * Cu	5.80	0.0531	0.8181
Natural Aging * Si * Cu	1.41	0.0129	0.9097
Natural Aging * Mg * Si *Cu	39.67	0.3634	0.5477
5% Strain * Natural Aging	2187.07	20.0368	< 0.0001
5% Strain * Natural Aging * Mg	685.50	6.2802	0.0135
5% Strain * Natural Aging * Si	3.61	0.0330	0.8561
5% Strain * Natural Aging * Mg * Si	20.26	0.1856	0.6673
5% Strain * Natural Aging * Cu	29.06	0.2662	0.6068
5% Strain * Natural Aging * Mg * Cu	54.90	0.5030	0.4795
5% Strain * Natural Aging * Si * Cu	4.54	0.0416	0.8387
5% Strain * Natural Aging * Mg * Si * Cu	1.74	0.0160	0.8997
Paint Bake (None)	9982.82	91.4577	< 0.0001
Paint Bake * Mg	150.43	1.3782	0.2426
Paint Bake * Si	392.13	3.5925	0.0603
Paint Bake * Mg * Si	47.39	0.4342	0.5111
Paint Bake * Cu	1166.98	10.6913	0.0014
Paint Bake * Mg * Cu	200.92	1.8407	0.1773
Paint Bake * Si * Cu	12.86	0.1178	0.7320
Paint Bake * Mg * Si * Cu	18.07	0.1656	0.6847
5% Strain * Paint Bake	5270.71	48.2876	< 0.0001

Term	Sum of Squares	F Ratio	Prob > F
5% Strain * Paint Bake * Mg	6.06	0.0555	0.8141
5% Strain * Paint Bake * Si	91.98	0.8427	0.3604
5% Strain * Paint Bake * Mg * Si	0.05	0.0005	0.9822
5% Strain * Paint Bake * Cu	25.82	0.2366	0.6275
5% Strain * Paint Bake * Mg * Cu	130.93	1.1995	0.2755
5% Strain * Paint Bake * Si * Cu	74.71	0.6845	0.4096
5% Strain * Paint Bake * Mg * Si * Cu	1.79	0.0164	0.8984
Paint Bake * Natural Aging	1736.71	15.9109	0.0001
Paint Bake * Natural Aging * Mg	390.42	3.5769	0.0608
Paint Bake * Natural Aging * Si	21.21	0.1943	0.6601
Paint Bake * Natural Aging * Mg * Si	14.98	0.1372	0.7117
Paint Bake * Natural Aging * Cu	465.10	4.2610	0.0410
Paint Bake * Natural Aging * Mg * Cu	52.68	0.4826	0.4885
Paint Bake * Natural Aging * Si * Cu	0.01	0.0000	0.9958
Paint Bake * Natural Aging * Mg * Si * Cu	61.44	0.5629	0.4545
5% Strain * Paint Bake * Natural Aging	156.33	1.4322	0.2336
5% Strain * Paint Bake * Natural Aging * Mg	191.50	1.7544	0.1887
5% Strain * Paint Bake * Natural Aging * Si	22.63	0.2073	0.6497

Term	Sum of Squares	F Ratio	Prob > F
5% Strain * Paint Bake * Natural Aging * Mg * Si	61.28	0.5614	0.4551
5% Strain * Paint Bake * Natural Aging * Cu	0.90	0.0082	0.9279
5% Strain * Paint Bake * Natural Aging * Mg * Cu	131.52	1.2049	0.2744
5% Strain * Paint Bake * Natural Aging * Si * Cu	44.02	0.4033	0.5265
5% Strain * Paint Bake * Natural Aging * Mg *Si * Cu	97.91	0.8970	0.3454